Time-Varying Jump Tails*

Tim Bollerslev† and Viktor Todorov ‡

First Version: February 18, 2013
This Version: August 22, 2013

Abstract

We develop new methods for the estimation of time-varying risk-neutral jump tails in asset returns. In contrast to existing procedures based on tightly parameterized models, our approach imposes much fewer structural assumptions, relying on extreme-value theory approximations together with short-maturity options. The new estimation approach explicitly allows the parameters characterizing the shape of the right and the left tails to differ, and importantly for the tail shape parameters to change over time. On implementing the procedures with a panel of S&P 500 options, our estimates clearly suggest the existence of highly statistically significant temporal variation in both of the tails. We further relate this temporal variation in the shape and the magnitude of the jump tails to the underlying return variation through the formulation of simple time series models for the tail parameters.

Keywords: Market risk; options; risk-neutral distributions; jumps; time-varying jump tails; extreme value theory.

JEL classification: C13, C14, G10, G12.

*We would like to thank Alok Bhargava (the Editor) and two anonymous referees for their many helpful comments, and Lai Xu for excellent research assistance. The research was supported by a grant from the NSF to the NBER, and CREATES funded by the Danish National Research Foundation (Bollerslev).

†Department of Economics, Duke University, Durham, NC 27708, and NBER and CREATES; e-mail: boller@duke.edu.

‡Department of Finance, Kellogg School of Management, Northwestern University, Evanston, IL 60208; e-mail: v-todorov@northwestern.edu.

1 Introduction

Financial asset returns are not conditionally normally distributed, but instead exhibit more slowly decaying, and often asymmetric, tails. This is true even over short horizons, as most easily seen from the presence of very pronounced volatility smiles for short maturity options.[1] These fatter than normal tails are directly attributable to occasionally large absolute price changes, or "jumps." The recent financial crises has further underscored the empirical relevance of tail events, and in turn econometric techniques for more accurately estimating and modeling such risks. We add to this literature through the development of new more flexible estimation procedures that explicitly allow for the possibility of time-varying tails for the large jump moves. In comparison to the existing literature, our approach imposes much fewer structural assumption, relying on extreme-value theory approximations together with short-maturity S&P 500 options. By focussing on the risk-neutral distributions implied from options data, our estimates speak directly to the jump tail risk that is priced by the market. Consistent with the existing literature, we find that the magnitude of the left jump tail associated with dramatic market declines far exceeds that of the right jump tail corresponding to large market appreciations.[2] Our new estimation procedures also clearly point to the existence of non-trivial predictable temporal dependencies in the tail index parameters characterizing the decay in both tails.

A number of previous studies have argued that the values of the parameters for the power laws governing the tails of return distributions may be subject to structural changes; see, e.g., the studies by Quintos et al. (2001) and Galbraith and Zernov (2004) based on the traditional Hill-estimator and daily aggregate equity index returns.[3] Relying on a large cross-section of stock returns, the more recent study by Kelly (2012) reinforces the idea of time-varying tail risks, and further argues that the temporal variation in the tail parameters may help understand aggregate market returns as well as cross-sectional differences in average returns.

[1]The failure of the traditional Black-Scholes model and the presence of volatility smiles after the market crash of 1987 is well documented in the asset pricing literature. The impact of this failure for econometric analysis in a corporate finance setting related to executive compensation has recently been studied by Bhargava (2013).

[2]The observation that the left tail inferred from aggregate equity index options dominates the right tail dates back at least to Rubinstein (1994), who attributed this to evidence of "crash-o-phobia."

[3]Fat tailed marginal daily return distributions may arise through stochastic volatility and leverage effects and/or or "jumps" possibly with time-varying intensity. As such, these earlier empirical studies are merely suggestive about the presence of temporal variation in the jump tail index.

Similarly, the study by Bollerslev and Todorov (2011a) demonstrates how high-frequency intraday data may be used in more accurately estimating dynamically evolving tails, and how these estimates may be used in more effective risk measurement and management decisions.

All of these studies are based on directly observed return data, and in turn pertain to the objective, or statistical, return distributions. By contrast, the new estimation procedures developed here pertain to the risk-neutral distribution, explicitly reflecting the way in which the market perceives and prices tail risks. The method builds on the insight that out-of-the-money short-maturity options effectively isolate the pricing of jump risk. Formally, in the limit for decreasing times-to-maturity and fixed moneyness, the diffusive risk will not affect the price of an out-of-the-money option. Regular variation in the jump tail measure, or compensator, therefore implies a one-to-one mapping between the shape of the jump tail measure and the slope of the option price surface in the strike dimension. Consequently, the tail index parameter may be uniquely identified, and in turn estimated, from a cross-section of deep out-of-the-money short-maturity options at a given point in time without making any assumptions about the temporal variation in the overall jump intensity process.[4]

The basic idea of inferring the risk-neutral jump tails from options is related to an earlier literature that seek to better explain option prices through jump risk; see, e.g., Bates (1996, 2000), Andersen et al. (2002), Pan (2002), Eraker (2004), Broadie et al. (2007), along with the more recent work by Christoffersen et al. (2012). All of these studies are based on specific, typically affine, parametric stochastic volatility jump diffusion models. Moreover, following Merton (1976), they postulate that conditionally on a jump occurring the size of the jump is normally distributed. Our approach is distinctly different in relying on a flexible nonparametric procedure that is able to accommodate complex dynamic tail dependencies and larger jump tails outside this classical Merton-framework.[5]

Our new estimation procedure is also related to the earlier work by Aït-Sahalia and Lo (1998), who non-parametrically estimate the entire risk-neutral state price density from options data. Their approach, however, explicitly assumes that the pricing kernel is time-

[4]A related estimation strategy has also been proposed in independent work by Hamidieh (2011).

[5]There is also a literature on Lévy-based option pricing outside the Merton-framework, in which the underlying price is modeled as an exponential-Lévy process (see, e.g., Cont and Tankov, 2004, and the references therein), or as a time-changed Lévy process (see, e.g., Carr et al., 2003). However, these studies generally impose tight parametric structures on the volatility process and the distributions of the jumps.

invariant. On the other hand, Rosenberg and Engle (2002) do allow the pricing kernel to change over time, but rely on tightly parameterized GARCH type models for describing the dynamic dependencies. Alternatively, Metaxoglou and Smith (2012) resort to the use of conditional quantile regression techniques for estimating time-varying pricing kernels. The recent study by Song and Xiu (2013) also explicitly relates the temporal variation in the risk-neutral distribution and the pricing kernel to the VIX index and the volatility of the aggregate market. Meanwhile, none of these estimation procedures are directly geared to the tails of the distribution. By contrast, our approach explicitly focusses on the tails and the tail decay parameters, in particular, ignoring other parts of the distribution.

The current paper is related to our earlier work, Bollerslev and Todorov (2011b), in which short-maturity option data is used to estimate semiparametrically risk-neutral jump tails. From an econometric point of view, however, there are two fundamental differences. First, unlike Bollerslev and Todorov (2011b) we explicitly allow the shape of the jump tails to vary over time. Second, the estimation in the present paper is based on a fixed time span and the entire cross-section of short maturity deep out-of-the-money options, whereas the estimation in Bollerslev and Todorov (2011b) rely on long time span asymptotics and only a limited number of strikes.

At a more general level, our empirical results are also related to the recent literature by Barro (2006) and others emphasizing the importance of incorporating rare disasters in macro-finance models. The idea that rare disasters, or tail events, may help explain the equity premium and other empirical puzzles in asset pricing dates back at least to Rietz (1988). Further building on these ideas, Gabaix (2012) and Wachter (2013) have recently shown that allowing for time-varying tail risks in otherwise standard equilibrium based asset pricing models may help explain the apparent excess volatility of aggregate equity index returns. Similarly, Bollerslev and Todorov (2011b) and Aït-Sahalia et al. (2013) suggest that much of the variance risk premium is directly attributable to disaster, or jump tail risk.

The plan for the rest of the paper is as follows. We begin in the next section with a discussion of the basic setup and assumptions, including our very general time-varying jump tail formulation. Section 3 discusses how options may be used for effectively separating jumps and continuous price variation, and outlines our new estimation procedures for the jump tail parameters. Section 4 summarizes the S&P 500 options data that we use in the estimation.

Our main empirical findings related to the tail risk parameters and the temporal variation therein are discussed in Section 5. Section 6 concludes. The proof of the key asymptotic approximation underlying our new estimation procedures is deferred to a technical Appendix.

2 Jump Tails

The continuous-time no-arbitrage framework that underly our new estimation procedure is very general. It includes all parametric models previously analyzed and estimated in the literature as special cases. We begin with a discussion of the basic setup and notation.

2.1 Setup and Assumptions

The underlying asset price X_t is defined on the filtered probability space $(\Omega, \mathcal{F}, \mathbb{P})$, where $(\mathcal{F}_t)_{t\geq 0}$ denotes the filtration. We assume the following general dynamic specification for X_t,

$$\frac{dX_t}{X_{t-}} = \alpha_t dt + \sigma_t dW_t + \int_{\mathbb{R}} (e^x - 1)\widetilde{\mu}(dt, dx), \tag{2.1}$$

where W_t is a Brownian motion, μ is a counting measure for the jumps in X with compensator $dt \otimes \nu_t(dx)$, so that $\widetilde{\mu}(dt, dx) = \mu(dt, dx) - dt\nu_t(dx)$ denotes the corresponding martingale measure under $\mathbb{P}$.[6][7] The drift and volatility processes, α_t and σ_t, respectively, are both assumed to have càdlàg paths, but otherwise left unspecified.

We will assume the existence of the alternative risk-neutral measure $\mathbb{Q}$ under which X_t follows the dynamics,

$$\frac{dX_t}{X_{t-}} = (r_t - \delta_t)dt + \sigma_t dW_t^{\mathbb{Q}} + \int_{\mathbb{R}} (e^x - 1)\widetilde{\mu}^{\mathbb{Q}}(ds, dx), \tag{2.2}$$

where r_t and δ_t denote the instantaneous risk-free rate and dividend yield of X_t, respectively, $W_t^{\mathbb{Q}}$ is a Brownian motion under $\mathbb{Q}$, and $\widetilde{\mu}^{\mathbb{Q}}(dt, dx) = \mu(dt, dx) - dt\nu_t^{\mathbb{Q}}(dx)$ where $dt \otimes \nu_t^{\mathbb{Q}}(dx)$ is the compensator of the jumps under $\mathbb{Q}$. The existence of $\mathbb{Q}$ follows directly from the lack of arbitrage under mild technical conditions (see, e.g., the discussion in Duffie, 2001). Of course, when the market is not complete, the risk-neutral measure is not unique. In the

[6] Recall $\mu([0,t], A) = \sum_{s\leq t} 1_{\{\log(\Delta X_s)\in A\}}$ for any measurable $A \in \mathbb{R}\setminus\{0\}$ and $\Delta X_s = X_s - X_{s-}$. Specific examples of jump compensators are given later in equations (2.7), (2.12) and (5.1).

[7] We have implicitly assumed that X_t does not have fixed times of discontinuities. This assumption is satisfied by virtually all asset pricing models hitherto used in the literature. Note also that μ is the counting measure for the jumps in $\log(X_t)$.

present analysis, however, we are only interested in the tail part of $\nu_t^{\mathbb{Q}}(dx)$. As explained further in Section 2.2 below, we will assume that this part of the distribution satisfies certain properties that allow for its unique identification from a set of short maturity options.

Our main interest centers on the tail component of the jump compensator, or the intensity of the jumps under $\mathbb{Q}$, and, in particular, the temporal variation therein. To be a valid jump compensator $\nu_t^{\mathbb{Q}}(dx)$ must satisfy (see, e.g., Proposition II.2.9 on p.77 of Jacod and Shiryaev, 2003),

$$\int_{\mathbb{R}} (x^2 \wedge 1)\nu_t^{\mathbb{Q}}(dx) < \infty, \quad \forall t \in \mathbb{R}_+, \tag{2.3}$$

which in terms of behavior in the tails is the same restriction as for a probability distribution.

Before proceeding with our analysis concerning the temporal variation in $\nu_t^{\mathbb{Q}}$, we introduce some additional notation. In particular, define the two functions,

$$\psi^+(x) = \begin{cases} e^x, & x > 0 \\ 0, & x \leq 0 \end{cases} \qquad \psi^-(x) = \begin{cases} e^{-x}, & x < 0 \\ 0, & x \geq 0 \end{cases}. \tag{2.4}$$

The transforms ψ^+ and ψ^- convert the jumps in the log-price into jumps in the price level. That is,

$$\frac{\Delta X_t}{X_{t-}} + 1 = \psi^+\left(\Delta \log(X_t)\right) 1_{\{\Delta \log(X_t) > 0\}} + \left[\psi^-\left(\Delta \log(X_t)\right)\right]^{-1} 1_{\{\Delta \log(X_t) < 0\}},$$

where $\Delta X_t = X_t - X_{t-}$ and $\Delta \log(X_t) = \log(X_t) - \log(X_{t-})$. Note also that the images of the measure $\nu_t^{\mathbb{Q}}$ under the mappings $x \to \psi^+(x)$ and $x \to \psi^-(x)$, respectively, may be expressed as,

$$\nu_{t,\psi}^{\mathbb{Q},+}(x) = \frac{\nu_t^{\mathbb{Q}}(\log(x))}{x}, \qquad \nu_{t,\psi}^{\mathbb{Q},-}(x) = \frac{\nu_t^{\mathbb{Q}}(-\log(x))}{x}, \quad \forall x > 1. \tag{2.5}$$

Finally, to further simplify the notation, let

$$\overline{\eta}^+(x) = \int_x^\infty \eta(du), \quad \forall x > 0, \qquad \overline{\eta}^-(x) = \int_{-\infty}^x \eta(du), \quad \forall x < 0. \tag{2.6}$$

denote the tail integrals for the arbitrary measure η on $\mathbb{R}$.

2.2 Time-Varying Jump Tails

Most of the models used in the asset pricing literature to date postulate the distribution of jumps to be time invariant. When temporal variation is allowed for, it is typically assumed that the dynamics in the risk-neutral tails may be characterized as,

$$\nu_t^{\mathbb{Q}}(dx) = \phi_t^+ \times \lambda^+(dx) 1_{\{x>0\}} + \phi_t^- \times \lambda^-(dx) 1_{\{x<0\}}, \tag{2.7}$$

where $\lambda^{\pm}$ are Lévy measures and $\phi_t^{\pm}$ some predictable processes.[8] For example, the double jump model of Duffie et al. (2000) employed in most of the empirical option pricing literature, or the time-changed tempered stable models of Carr et al. (2003), both satisfy (2.7). In these models, it is also typically assumed that the temporal variation in the left and the right tails may be described by the same process, so that $\phi_t^+ = \phi_t^-$. Moreover the temporal variation is typically assumed to be an affine function of the diffusive volatility σ_t^2.

The standard modeling assumption for the jump intensity in (2.7) severely constrains the behavior of the jump tails. In particular, recalling the notation in (2.6), it is easy to see that (2.7) implies,

$$\frac{\overline{\nu}_t^{\mathbb{Q},+}(x)}{\overline{\nu}_t^{\mathbb{Q},+}(y)} = \frac{\overline{\lambda}^{+}(x)}{\overline{\lambda}^{+}(y)}, \quad \forall\, x > y > 0, \qquad \text{and} \qquad \frac{\overline{\nu}_t^{\mathbb{Q},-}(x)}{\overline{\nu}_t^{\mathbb{Q},-}(y)} = \frac{\overline{\lambda}^{-}(x)}{\overline{\lambda}^{-}(y)}, \quad \forall\, x < y < 0, \tag{2.8}$$

so that the relative importance of differently sized jumps is time invariant. As such, the only way for the intensity of large sized jumps to increase (decrease) over time is for the intensity of *all* sized jumps to simultaneously increase (decrease) over time.

This implication of the standard approach to jump modeling is further illustrated in Figure 1, which plots the left and right jump tails for two different values of the ϕ_t^+ and ϕ_t^- "parameters." Since the shape of the tails remain constant, only proportional changes in the intensities are allowed for over time.

The traditional modeling assumption in (2.7) also implies that the behavior of the jump tails depends exclusively on the tail behavior of the time-invariant measure λ. Even though λ isn't formally a probability measure, and may explode around zero, the restriction in (2.3) ensures that the measure behaves like a probability measure outside of zero. Following Bollerslev and Todorov (2011a), we will assume that the corresponding tail measures $\overline{\lambda}_{\psi}^{\pm}$ belong to the maximum domain of attraction of an extreme value distribution, where the two measures $\lambda_{\psi}^{+}(x)$ and $\lambda_{\psi}^{-}(x)$ are naturally defined from $\lambda^{\pm}$ as in (2.5). We will restrict our attention to the empirically relevant case, when the extreme value distribution is of the Frechet type (see, e.g., Theorem 3.3.7 in Embrechts et al., 2001),

$$\overline{\lambda}_{\psi}^{\pm}(x) = x^{-\alpha^{\pm}} L^{\pm}(x), \quad \alpha^{\pm} > 0, \tag{2.9}$$

[8] Let $X_t^{(d)}$ denote the jump component of X_t. The model in (2.7) is then equivalent to $X_t^{(d)}$ having a representation of a sum of time-changed Lévy processes (see Theorem 10.27 in Jacod, 1979). That is, there exist Lévy processes L_t^+ and L_t^- with Lévy measures λ^+ and λ^- such that for $X_t^{(d)}$ with compensator defined in (2.7), $X_t^{(d)} = L_{T_t^+}^+ + L_{T_t^-}^-$ for $T_t^+ = \int_0^t \phi_s^+ ds$ and $T_t^- = \int_0^t \phi_s^- ds$.

where $L^{\pm}(x)$ are slow-varying at infinity functions.[9] It is then possible to show that,

$$\frac{\overline{\lambda}_{\psi}^{\pm}(u+x)}{\overline{\lambda}_{\psi}^{\pm}(x)} \approx \left(\frac{x+u}{x}\right)^{-\alpha^{\pm}}, \quad x>0,\ u>0, \tag{2.10}$$

where the approximation arises from the presence of the slowly-varying function in (2.9) (see Bollerslev and Todorov, 2011a, and the references therein for more details). Combining the model for the jump intensity in (2.7) with the tail approximation for $\overline{\lambda}^{\pm}$ in (2.10), it follows that

$$\frac{\overline{\nu}_{t,\psi}^{\mathbb{Q},\pm}(x)}{\overline{\nu}_{t,\psi}^{\mathbb{Q},\pm}(y)} \approx \left(\frac{x}{y}\right)^{-\alpha^{\pm}}, \quad x>y>1. \tag{2.11}$$

Hence, this ratio of the jump tail intensities is also time-invariant, with a power low decay determined by the maximum domain of attraction of $\overline{\lambda}^{\pm}$.

To help fix ideas, consider the double-exponential jump model applied by Kou (2002) and Kou and Wang (2002) among others,

$$\lambda^{+}(x) = c^{+}e^{-\alpha^{+}x}1_{\{x>0\}}, \quad \lambda^{-}(x) = c^{-}e^{-\alpha^{-}|x|}1_{\{x<0\}}, \quad \alpha^{\pm}>0, \quad c^{\pm}\geq 0. \tag{2.12}$$

It follows readily that for this model,

$$\overline{\lambda}_{\psi}^{+}(x) = \frac{c^{+}}{\alpha^{+}}x^{-\alpha^{+}}, \qquad \overline{\lambda}_{\psi}^{-}(x) = \frac{c^{-}}{\alpha^{-}}x^{-\alpha^{-}}, \qquad \forall x>1. \tag{2.13}$$

Hence, equation (2.9) holds with $L^{\pm}(x) = \frac{c^{\pm}}{\alpha^{\pm}}$ being constant, and therefore all of the subsequent approximations hold exactly for the double-exponential model. Of course, for most other jump models of the form (2.7), the corresponding expressions will only hold approximately with $\overline{\lambda}_{\psi}^{\pm}$ in the domain of attraction of a Frechet extreme value distribution.[10]

Even though (2.7) encompasses most jump models hitherto employed in the literature, and in empirical finance in particular, as the discussion above illustrates, this specification does entail some rather stringent assumptions in regards to the temporal variation, or the lack thereof, in the jump tails. In particular, there is no apriori reason to expect that the shape of the tails stays constant over time. On the contrary, with financial data one might

[9]Recall that a function $L(x)$ is said to be slowly varying at infinity if $\lim_{x\to\infty}\frac{L(vx)}{L(x)}=1,\ \forall v>0$.

[10]An example is the tempered stable jump process with $\lambda^{\pm}(x)$ in (2.7) given by $\lambda^{+}(x) = c^{+}\frac{e^{-\alpha^{+}x}}{x^{1+\beta^{+}}}1_{\{x>0\}}$ and $\lambda^{-}(x) = c^{-}\frac{e^{-\alpha^{-}|x|}}{|x|^{1+\beta^{-}}}1_{\{x<0\}}$ for $\beta^{\pm}<2$. It is easy to check that for this process, (2.9) continues to hold, albeit with some more complicated functions $L^{\pm}(x)$.

naturally expect that the magnitude and the shape of the tails, and in turn the tail decay parameters, respond to economic conditions and change over time.

In an effort to accommodate richer tail behaviors, we therefore consider the following generalization of the standard jump intensity process,[11]

$$\nu_t^{\mathbb{Q}}(dx) = \left(\phi_t^+ \times e^{-\alpha_t^+ x} 1_{\{x>0\}} + \phi_t^- \times e^{-\alpha_t^- |x|} 1_{\{x<0\}}\right) dx. \tag{2.14}$$

This generalization of (2.7) explicitly allows for two separate sources of variation in the jump tails, in the form of level shifts of the intensity governed by $\phi_t^{\pm}$, and shifts in the rate of decay of the tails governed by $\alpha_t^{\pm}$. Correspondingly, the expression for $\overline{\lambda}_{\psi}^{\pm}$ in (2.9) generalizes to,

$$\overline{\lambda}_{t,\psi}^{\pm}(x) \propto x^{-\alpha_t^{\pm}}, \qquad \alpha_t^{\pm} > 0, \quad x \to \infty. \tag{2.15}$$

This in turn implies that the ratio of the jump intensities on the left-hand-side of equation (2.11) is no longer constant,

$$\frac{\overline{\nu}_{t,\psi}^{\mathbb{Q},\pm}(x)}{\overline{\nu}_{t,\psi}^{\mathbb{Q},\pm}(y)} = \left(\frac{x}{y}\right)^{-\alpha_t^{\pm}}, \qquad x > y > 1, \tag{2.16}$$

but instead depends on the values of the possibly time-varying $\alpha_t^{\pm}$ processes.

To illustrate, consider Figure 2, which plots the left and right jump tails for a representative jump process of the form (2.14) for identical values of $\phi_t^{\pm}$, but different values of $\alpha_t^{\pm}$. In comparison to the previous Figure 1, which restricts the shape of the tails to be time-invariant, allowing for different values of $\alpha_t^{\pm}$ clearly affords an added flexibility for empirically modeling time-varying jump tail risks.

3 Risk-neutral jump tail estimation

Option prices explicitly incorporate the risk-neutral expectations of tail events. Deep out-of-the-money close-to-maturity options, in particular, effectively render key features of the risk-neutral jump intensity process estimable. This greatly facilitates tail estimation by avoiding the need for large numbers of actual tail realizations.[12] We begin our discussion of the estimation procedures by considering the case of time-invariant jump tails.

[11] Similar results to the ones derived below could be obtained at the cost of additional technical complications by only requiring the *tail* component of $\nu_t^{\mathbb{Q}}(dx)$ to adhere to the structure in (2.14).

[12] As previously noted, the expectations inherent in options data also pertain directly to the risk-neutral distribution of practical relevance from a pricing perspective.

To set the notation, let $O_{t,\tau}(k)$ denote the time t price of an out-of-the-money option on X_t with time to expiration τ and log-moneyness $k = \log(K/F_{t-,\tau})$, where $F_{t,\tau}$ refers to the futures price of X_t, and K denotes the strike of the option.[13] Following Bollerslev and Todorov (2011b) it is possible to show that for the baseline jump intensity process in equation (2.7),

$$\frac{e^{r_{t,\tau}} O_{t,\tau}(k)}{F_{t-,\tau}} \approx \begin{cases} \int_t^{t+\tau} \int_{\mathbb{R}} (e^x - e^k)^+ \mathbb{E}_t^{\mathbb{Q}}(\nu_s^{\mathbb{Q}}(dx)) ds, & \text{if } k > 0, \\ \int_t^{t+\tau} \int_{\mathbb{R}} (e^k - e^x)^+ \mathbb{E}_t^{\mathbb{Q}}(\nu_s^{\mathbb{Q}}(dx)) ds, & \text{if } k < 0, \end{cases} \tag{3.1}$$

where $e^{r_{t,\tau}} = \mathbb{E}_t^{\mathbb{Q}}\left(e^{\int_t^{t+\tau} r_s ds}\right)$ denotes the risk-free interest rate over the $[t, t+\tau]$ time-interval. This approximation formally relies on $\tau \downarrow 0$ and $k \to \pm\infty$. However, the approximation error is quite small for the maturity times and moneyness employed in the empirical analysis below, and we will consequently ignore this error in the sequel.[14]

Combining (3.1) with the extreme value approximations for the baseline jump intensity process, it follows that

$$\frac{e^{r_{t,\tau}} O_{t,\tau}(k)}{\tau F_{t-,\tau}} \approx (\phi_t^+ 1_{\{k>0\}} + \phi_t^- 1_{\{k<0\}}) \Phi(\alpha^{\pm}, tr, k), \tag{3.2}$$

where

$$\Phi(\alpha^{\pm}, tr, k) = \begin{cases} \frac{\overline{\lambda}_\psi^+(tr)}{\alpha^+ - 1} \frac{\left(e^k\right)^{1-\alpha^+}}{tr^{-\alpha^+}}, & e^k \geq tr > 1, \\ \frac{\overline{\lambda}_\psi^-(tr)}{\alpha^- + 1} \frac{\left(e^{-k}\right)^{-1-\alpha^-}}{tr^{-\alpha^-}}, & e^{-k} \geq tr > 1, \end{cases} \tag{3.3}$$

for some threshold $tr > 1$. Going one step further, this implies that the time-varying $\phi_t^{\pm}$ processes are purged from the ratio of the logarithmic prices for the same maturity options with different strikes. Specifically, consider two options with the same maturity τ, but different moneyness $k_1 < k_2$,

$$\log\left(\frac{O_{t,\tau}(k_2)}{O_{t,\tau}(k_1)}\right) = \begin{cases} (1-\alpha^+)(k_2 - k_1), & e^{k_2} > e^{k_1} > tr, \\ (1+\alpha^-)(k_2 - k_1), & e^{-k_2} > e^{-k_1} > tr. \end{cases} \tag{3.4}$$

Consequently, the time-invariant tail index parameters $\alpha^{\pm}$ may be consistently estimated in a nonparametric fashion from an ever increasing number of short-maturity options with

[13] By definition $O_{t,\tau}(k)$ represents a call (put) option for $k > 0$ ($k < 0$).

[14] There are several sources of the approximation error. One is the time variation in the risk-neutral jump measure as well as the time variation in the diffusive stochastic volatility. Second is the occurrence of more than one large jump before the expiration of the option. Finally, there is an error due to the sole presence of a diffusive component. The first two errors are quite negligible for the models typically estimated in the literature. Footnote 22 below explains how it is possible to directly incorporate the source of the third approximation error; i.e., the presence of a diffusion in the price with constant volatility at the current spot level. Further discussion and Monte Carlo simulation-based evidence pertaining to the size of these approximation errors are reported in Bollerslev and Todorov (2011b).

deeper strikes, or an ever increasing number of options over an increasing sample span T, or both.

In the first set of results reported on below, we rely on the following simple estimators,

$$\begin{aligned}\widehat{\alpha}^{+} &= \text{argmin}_{\alpha^{+}} \frac{1}{\sum_{t=1}^{T} N_t^{+}} \sum_{t=1}^{T} \sum_{i=2}^{N_t^{+}} g\left(\frac{\log\left(\frac{O_{t,\tau_t}(k_{t,i})}{O_{t,\tau}(k_{t,i-1})} \right)}{k_{t,i}-k_{t,i-1}} - (1-\alpha^{+}) \right), \\ \widehat{\alpha}^{-} &= \text{argmin}_{\alpha^{-}} \frac{1}{\sum_{t=1}^{T} N_t^{-}} \sum_{t=1}^{T} \sum_{i=2}^{N_t^{-}} g\left(\frac{\log\left(\frac{O_{t,\tau_t}(k_{t,i})}{O_{t,\tau}(k_{t,i-1})} \right)}{k_{t,i}-k_{t,i-1}} - (1+\alpha^{-}) \right),\end{aligned} \tag{3.5}$$

where N_t^{+} (N_t^{-}) denotes the total number of calls (puts) on day t with moneyness $0 < k_{t,1} < ... < k_{t,N_t^{+}}$ ($0 < -k_{t,1} < ... < -k_{t,N_t^{-}}$) used in the estimation of $\widehat{\alpha}^{+}$ ($\widehat{\alpha}^{-}$). The choice of the function $g : \mathbb{R} \to \mathbb{R}_{+}$, with the property that $g(x) = 0$ iff $x = 0$, is naturally dictated by the assumption about the log-option pricing errors. In particular, assuming that the errors have a median of zero conditional on the filtration of the original probability space suggests a Least Absolute Deviation (LAD) type estimator and $g(x) = |x|$.

Two alternative asymptotic schemes naturally suggest themselves for characterizing the distributions of $\widehat{\alpha}^{\pm}$. First, consider the case in which $T \to \infty$ and $N_t^{\pm}$ is fixed.[15] In this situation, ignoring the approximation error in (3.2), consistency and asymptotic normality for $\widehat{\alpha}^{\pm}$ follows readily under standard ergodicity and mixing conditions about the temporal dependencies in the option errors. Alternatively, consider the asymptotic setting in which T is fixed and $N_t^{\pm} \to \infty$. This setup mirrors the one analyzed in Andersen et al. (2013) for the estimation of specific parametric pricing models based on a panel of options over a fixed time span. In this situation, the estimator in (3.5) will require that the errors are averaged out spatially, so that we will need for the option-errors to be at most weakly dependent across strikes.[16] Then, again ignoring the approximation error in (3.2), consistency and asymptotic normality follow readily from the results in Andersen et al. (2013), with the limiting distribution of the parameter estimates now mixed Gaussian.

[15] In fact, $N_t^{\pm} = 2$ suffice as there is only one parameter to be estimated for each of the two tails.

[16] Earlier work allowing for option price errors have typically relied on strong parametric assumptions regarding the errors. Adopting the spatial averaging approach of Andersen et al. (2013) allows us to be nonparametric about the option errors, while accommodating possible dependence between the errors and the price process as well as any underlying latent state variables driving volatility and jump intensity. A restriction, however, is that the option errors have limited dependence in the cross-section. If out-of-the-money close-to-maturity options had a common error component in the cross-section, spatial averaging would not help to eliminate the effect of the errors, and the errors would need to be explicitly incorporated into the pricing model; Bates (2000) also refers to such errors as "model specification errors."

The flexibility of our estimator in (3.5) with respect to the observation scheme, i.e., its ability to work both in settings with increasing time span and/or increasing cross-sections of options, stems from the use of the moment conditions in (3.4), which conveniently avoid inference about $\phi_t^{\pm}$. By contrast, the approach developed in Bollerslev and Todorov (2011b) works only for increasing time span, or $T \to \infty$.[17]

The approximations underlying (3.5) are based on the standard jump specification in (2.7) and the assumption that the tail index parameters do nor change over time. Instead, consider the more general jump intensity process in (2.14) explicitly allowing $\alpha_t^{\pm}$ to be time-varying. In this situation, it follows from Lemma 1 shown in the Appendix that

$$\frac{e^{r_{t,\tau}} O_{t,\tau}(k)}{F_{t-,\tau}} \approx \begin{cases} \frac{\tau \phi_t^+ e^{k(1-\alpha_t^+)}}{\alpha_t^+(\alpha_t^+ - 1)}, & \text{if } k > 0, \\ \frac{\tau \phi_t^- e^{k(1+\alpha_t^-)}}{\alpha_t^-(\alpha_t^- + 1)}, & \text{if } k < 0, \end{cases} \tag{3.6}$$

for $\tau \downarrow 0$. Note that for $\alpha_s^{\pm} = \alpha_t^{\pm}$ and $\phi_s^{\pm} = \phi_t^{\pm}$ for all $s \in [t, t+\tau]$, the right-hand side of (3.6) trivially equals the right-hand side of (3.1). In general, however, the right hand-side of (3.6), and in turn the ratio in (3.4) forming the basis for the estimator in (3.5), will depend on the time-varying jump tail parameters.

However, assuming that the time-variation in the tail index parameters are of smaller order of magnitude than the variation in the right-hand side of (3.6), the ratio of the logarithmic option prices may still be used in estimating $\alpha_t^{\pm}$. In particular, by similar arguments to the ones underling (3.5), it follows that

$$\begin{aligned} \widehat{\alpha}_t^+ &= \text{argmin}_{\alpha_t^+} \tfrac{1}{N_t^+} \textstyle\sum_{i=2}^{N_t^+} g\left(\frac{\log\left(\frac{O_{t,\tau_t}(k_{t,i})}{O_{t,\tau}(k_{t,i-1})}\right)}{k_{t,i} - k_{t,i-1}} - \left(1 - \alpha_t^+\right) \right), \\ \widehat{\alpha}_t^- &= \text{argmin}_{\alpha_t^-} \tfrac{1}{N_t^-} \textstyle\sum_{i=2}^{N_t^-} g\left(\frac{\log\left(\frac{O_{t,\tau_t}(k_{t,i})}{O_{t,\tau}(k_{t,i-1})}\right)}{k_{t,i} - k_{t,i-1}} - \left(1 + \alpha_t^-\right) \right), \end{aligned} \tag{3.7}$$

consistently estimates $\alpha_t^{\pm}$ for $t = 1, 2, ..., T$ when $N_t^{\pm} \to \infty$ (with an associated CLT exactly as before). Importantly, these estimates for the time-varying tail shape parameters put no

[17] The alternative GMM estimator for $\alpha^{\pm}$ in Bollerslev and Todorov (2011b) is based on the moment conditions,

$$m(\mu^{\pm}, \alpha^{\pm}, \mathbf{k}) = \frac{1}{T} \sum_{t=1}^{T} \frac{e^{r_{t,\tau_t}} O_{t,\tau_t}(\mathbf{k})}{F_{t-,\tau}} - \mu^{\pm} \times \Phi(\alpha^{\pm}, tr, \mathbf{k}),$$

where $\mu^{\pm} = \mathbb{E}\left(\phi_t^{\pm}\right)$, and $\Phi(\alpha^{\pm}, tr, \mathbf{k})$ denotes the vector with elements $\Phi(\alpha^{\pm}, tr, k_i)$ for different strikes $(k_i)_{i=1,...,d}$.

restrictions on the scale parameters $\phi_t^{\pm}$ that shift the whole Lévy density through time. Obviously, due to the time-variation in our parameters of interest, $\alpha_t^{\pm}$, the above estimators in (3.7) will not work in the long span setting with $N_t^{\pm}$ fixed.[18]

In practice, of course, we do not have an infinite number of options with different strikes at each point in time. Thus, as a compromise, for the empirical results reported on below we estimate time-varying annual, monthly, and weekly tail shape parameters by summing the right-hand-side of the objective function in (3.7) over the relevant horizons. This inevitably limits our ability to recover any temporal variation in $\alpha_t^{\pm}$ at higher frequencies. More formally, this "pooling" of the option data also means that we are recovering an average of the tail shape parameters over the relevant time-intervals.[19] We turn next to a discussion of the actual options data that we use in implementing these estimators.

4 Data

The options data that we use in our analysis is obtained from OptionMetrics. The raw data consists of closing bid and ask quotes for all S&P 500 options traded on the Chicago Board of Options Exchange (CBOE). The data span the period from January 1996 to December 2011, for a total of $4,027$ trading days.

Following standard procedures in the option pricing literature our "cleaning" of the data is comprised of several steps. To begin, we keep only out-of-the-money options with positive bid prices. Further, to rule out arbitrage, starting with the closest at-the-money options we only keep the subsequent (in the strike dimension) out-of-the-money puts and calls with lower midquotes.[20] If this monotonicity condition is violated for a given pair of midquotes, we retain the option with the highest volume, and in the event of identical volume the option that is closest to being at-the-money. Lastly, to alleviate potential market microstructure complications, we only consider options with at least eight calendar days to expiration. The resulting sample underlying our empirical analysis is summarized in Table 1 in terms of the average number of options available per trading day as a function of moneyness.

[18]Similarly, the standard GMM estimator of Bollerslev and Todorov (2011b) based on $T \to \infty$ would, of course, no longer be applicable in the case when $\alpha_t^{\pm}$ varies over time.

[19]For least squares, i.e., $g(x) = x^2$, the estimates would be interpretable as a simple average.

[20]That is, the no-arbitrage condition that we enforce for the observed midquotes is the monotonicity of the option price in the strike dimension.

In our parametric modeling, we also rely on so-called realized variation measures, first popularized by Andersen and Bollerslev (1998), Andersen et al. (2001) and Barndorff-Nielsen and Shephard (2002). Our construction of these measures is based on intraday S&P 500 returns calculated from futures prices obtained from Tick Data Inc. The prices are recorded at five-minute intervals, with the first price of the day at 8:35 (CST) until the last price of the day at 15:15, for a total of 81 intraday price observations per trading day.

5 Empirical modeling of jump tails

Our estimators for the tail index parameters in (3.5) and (3.7) both rely on the use of close-to-maturity out-of-the-money options to assess the jump tail risk. In practice, of course, the price of the options will invariably reflect some diffusive risk as well. Intuitively, the larger the diffusive volatility, the larger the impact of the diffusive price component, especially when the (priced) jump risk does not increase with the volatility. In order to help mitigating this effect, for the estimation of the left (right) tail parameters reported on below we only use put (call) options with log-moneyness below (above) $-2.5 \times \sigma_t^{ATM}\sqrt{\tau}$ ($1.0 \times \sigma_t^{ATM}\sqrt{\tau}$), where σ_t^{ATM} denotes the at-the-money Black-Scholes implied volatility. By explicitly relating the threshold of the moneyness for the options used in the estimation to the overall level of the volatility, we screen out more relatively close to at-the-money options in periods of high volatility, thereby effectively minimizing the impact of the on average larger diffusive price component when the volatility is high.[21]

5.1 Are the shapes of the jump tails time-invariant?

We begin our empirical analysis by estimating the tail index parameters under the assumption that the jump tails are time invariant over annual, monthly, and weekly horizons. Figures 3 and 4 show confidence bounds for the resulting non-overlapping estimates for the left and right tail index parameters, $\widehat{\alpha}_t^+$ and $\widehat{\alpha}_t^-$, respectively. In addition, we also include the estimates for $\alpha^{\pm}$ obtained by assuming that the shapes of the jump tails remain constant

[21] The result in (3.2), as shown in Lemma 1 in the Appendix, formally holds for a fixed strike, as opposed to a strike that shrinks asymptotically with $\tau \downarrow 0$. Our choice of threshold for the moneyness jointly depending on τ and σ_t^{ATM} is merely a convenient way of empirically accounting for time-varying volatility, and should not be interpreted asymptotically. In the empirical application, of course, we also work with (approximately) the same $\tau > 0$ throughout.

throughout the whole sample, as indicated by the horizontal lines in Figures 3 and 4.

The estimates obtained by pooling the options over annually frequencies, reported in the top two panels, are naturally very smooth. Even at that low frequency, however, there are still clearly discernable patterns in the estimates, with fatter tails during the recent 2008-09 financial crises, and to a lesser extend 2001-02. Also, both of the tails appear thinner in the relatively quiet 2004-07 period. Of course, the magnitude of the estimates for the left tail parameters far exceed the right tail estimates.

Turning to the monthly estimates reported in the middle panel in the two figures, these same general patterns stand out more clearly. In particular, allowing for the shape of the jump tails to change on a monthly as opposed to an annual basis appears especially important for capturing large changes in the tail parameters during the 2008-09 financial crisis, as well as the more turbulent 1998-99 and 2001-02 time periods. Allowing for the left and right tail parameters to change at weekly frequency further reinforces and magnifies this temporal variation in the shapes of the jump tails. Of course, the use of only weekly data also results in more "noisy" point estimates. In the next section we explore the use of simple parametric time series models as a way to help "smooth" out this estimation error and further understand the driving forces behind the dynamic dependencies in the weekly $\alpha_t^{\pm}$ tail parameters.

In order to further highlight the importance of allowing for time-varying jump tails, it is instructive to consider the implications for correctly pricing the options across different strikes. To this end, we plot in Figure 5 the relative fit for $\log(O_{t,\tau_t}(k_{t,1})/O_{t,\tau_t}(k_{t,N_t^{\pm}}))$ averaged over weeks based on our annual, monthly, and weekly estimates for $\alpha_t^{\pm}$. This particular ratio of option prices represents the rate of decay from the closest to at-the-money to the deepest out-of-the-money short-maturity options used in the estimation.

As seen from Figure 5, ignoring the time variation in the tails can have a rather detrimental effect in terms of the ability to account for the time-varying slope of the short-maturity option surface. Forcing the tail index to be constant over the entire sample or annual frequencies can result in severe over-estimation of the observed option decay in periods of market distress, as most clearly seen during the 2008-09 financial crises. By contrast, the estimation errors associated with the monthly tail estimates appear homogenous throughout the sample. The weekly tail estimates even further improve the fit, as seen by the drop in the magnitude of the errors as well as their persistence over time. Most remarkably, the

errors associated with fitting the option surface slope in 1998-99 and 2008-09 are of the same magnitude as the errors in other time periods.

A closer look at the weekly errors in Figure 5 also shows that whereas the model in (2.14) affords an approximately unbiased fit to the slope of the out-of-the-money put decay, the errors in fitting the slope of the out-of-the-money call decay are slightly downward biased. This slight over-estimation of the actual call option decay may be attributed to the impact of the diffusive price component. In particular, from the summary numbers in Table 1 the general availability of options necessitates the use of relatively closer to at-the money calls than puts, thereby "contaminating" the identification of the true right jump tail.[22] Of course, as previously noted, the left jump tail is also orders of magnitude larger than the right tail.

As a final gauge for the improvements afforded by the more flexible jump specification in (2.14), we also compare the fit with that of the standard finite activity jump model with normally distributed jump sizes pioneered by Merton (1976). The Lévy density for the generalized Merton jump model, used extensively in the empirical and theoretical asset pricing literature, may be expressed as,[23]

$$\nu_t^{\mathbb{Q}}(dx) = \phi_t \times \frac{e^{-\frac{(x-\mu)^2}{2\sigma^2}}}{\sqrt{2\pi\sigma^2}} dx. \tag{5.1}$$

It follows readily that for this model,

$$\frac{e^{r_{t,\tau}} O_{t,\tau}(k)}{\tau F_{t-,\tau}} \approx \phi_t \Psi(k, \mu, \sigma^2), \tag{5.2}$$

[22]Relating the truncation levels for the options used in the estimation to the overall level of the volatility helps alleviate this effect. In addition, we also experimented with explicitly adjusting for the diffusive price component through the refined approximation,

$$\frac{e^{r_{t,\tau}} O_{t,\tau}(k)}{\tau F_{t-,\tau}} \approx \begin{cases} \phi_t^+ \int_{\mathbb{R}} \int_{\mathbb{R}} \left(e^{x + z\sigma_t\sqrt{\tau}} - e^k \right)^+ e^{-\alpha_t^+ |x|} \frac{e^{-z^2/2}}{\sqrt{2\pi}} dx dz, & k > 0, \\ \phi_t^- \int_{\mathbb{R}} \int_{\mathbb{R}} \left(e^k - e^{x + z\sigma_t\sqrt{\tau}} \right)^+ e^{-\alpha_t^- |x|} \frac{e^{-z^2/2}}{\sqrt{2\pi}} dx dz, & k < 0, \end{cases}$$

with σ_t approximated by $QV^c_{(t-1,t]}$ (see equation (5.6) in the next subsection and the discussion afterwards for its measurement from high-frequency data). The estimation results for the left tails and the weekly α_t^- were essentially unaltered compared to the estimates shown in the bottom panel in Figure 3. For the right tails this refinement did result in slightly lower estimates for α_t^+ compared to ones shown in the bottom panel in Figure 4. Further details concerning these results are available upon request.

[23]The original Merton jump-diffusion model, of course, postulates that ϕ_t is constant. Also, the fact that the model in (2.14) allows the left and right jump tail intensities to differ, plays no role in our comparisons of the two models which focuses on the jump distribution, or rather the tail part of it, and the fit of the option decay in the moneyness dimension for short maturity options.

where

$$\Psi(k,\mu,\sigma^2) = \begin{cases} e^k \Phi\left(\frac{k-\mu}{\sigma}\right) - e^{\mu+\sigma^2/2}\Phi\left(\frac{k-\mu-\sigma^2}{\sigma}\right), & k<0, \\ e^{\mu+\sigma^2/2}\left(1-\Phi\left(\frac{k-\mu-\sigma^2}{\sigma}\right)\right) - e^k\left(1-\Phi\left(\frac{k-\mu}{\sigma}\right)\right), & k>0. \end{cases} \tag{5.3}$$

This in turn implies that the rate of decay in the jump tails "accelerates" the deeper out of the money the options get. Consequently, the slope defined by $\frac{1}{k_2-k_1}\log\left(O_{t,\tau}(k_2)/O_{t,\tau}(k_1)\right)$, will depend on the strikes of the options, or k_1 and k_2. By contrast, for the jump specification in (2.14) this ratio remains the same for all strikes, and only depends on the tail shape parameters $\alpha_t^{\pm}$.

To help directly illustrate this, we estimate the Merton jump model on a weekly basis,[24]

$$\begin{aligned}(\widehat{\mu}_t,\ \widehat{\sigma}_t{}^2) = \text{argmin}_{(\mu_t,\sigma_t^2)}\Bigg\{ & \frac{1}{N_t^+}\sum_{i=2}^{N_t^+} g\left(\log\left(\frac{O_{t,\tau_t}(k_{t,i})}{O_{t,\tau}(k_{t,i-1})}\right) - \log\left(\frac{\Psi(k_{t,i},\mu_t,\sigma_t^2)}{\Psi(k_{t,i-1},\mu_t,\sigma_t^2)}\right)\right), \\ & + \frac{1}{N_t^-}\sum_{i=2}^{N_t^-} g\left(\log\left(\frac{O_{t,\tau_t}(k_{t,i})}{O_{t,\tau}(k_{t,i-1})}\right) - \log\left(\frac{\Psi(k_{t,i},\mu_t,\sigma_t^2)}{\Psi(k_{t,i-1},\mu_t,\sigma_t^2)}\right)\right)\Bigg\},\end{aligned} \tag{5.4}$$

where in parallel to our time-varying estimates of $\alpha_t^{\pm}$ based on (3.7) discussed above, we rely on all of the options within a week. Figure 6 plots the resulting weekly fits to the slope of the short-maturity option surface, as given by $\log(O_{t,\tau_t}(k_{t,1})/O_{t,\tau_t}(k_{t,N_t^{\pm}}))$. Comparing the magnitude of these errors to the weekly errors in the bottom two panels in Figure 5, the alternative jump specification in (2.14) clearly provides the superior fit.[25] Moreover, the errors from fitting the option tail decay by the light-tailed Merton jump model are also serially correlated, further highlighting the inadequacy of that traditional approach.

We conclude that both the shape and the temporal variation in the shape parameters are important for satisfactorily describing the risk-neutral distributions and the dynamics in the options-implied jump tails. We turn next to a simple parametric model for describing these dynamic dependencies as embodied in our time-varying $\widehat{\alpha}_t^{\pm}$ parameter estimates.

[24]Of course, the Merton model as traditionally implemented in the literature restricts the parameters to be constant for the whole sample.

[25]Note, the Merton model and the jump specification in (2.14) both involve two parameters for describing the shape of the tails. Both jump specifications also allow for asymmetric jump distributions; in the Merton model this is controlled by the mean parameter μ_t.

5.2 Parametric modeling

Our nonparametric estimation procedures entail very minimal assumptions. Not surprisingly, the resulting parameter estimates for $\alpha_t^{\pm}$ reported in Figures 3 and 4 also appear somewhat "noisy," especially at the higher weekly frequency. Parametric modeling of the time-variation in the tail index parameters provides a way to "regularize" the sample path by imposing more structure on the variation in the estimates. For concreteness, we will focus on the weekly frequency, but the same ideas could be applied to any discrete-time horizon.

The nonparametric weekly estimates, shown in the bottom two panels in Figures 3 and 4, clearly point to important own serial dependencies. As such, this naturally suggests the use of an autoregressive type model structure.[26] In addition, existing empirical findings pertaining to the parametric affine jump-diffusion class of models indirectly suggest that the shape of the jump tails might be related to the level of the volatility, or the quadratic variation of the underlying price process. To empirically explore the strength of these relations, we postulate the following simple specification,

$$\alpha_j^{\pm} = \beta_0^{\pm} + \beta_1^{\pm}\alpha_{j-1}^{\pm} + \beta_2^{\pm}\log(1 + QV^c_{(\tau_{j-1},\tau_j]}) + \beta_3^{\pm}\log(1 + QV^d_{(\tau_{j-1},\tau_j]}) + \epsilon_j^{\pm}, \tag{5.5}$$

where $j = 1, ..., J$ refers to the different weeks in the sample, and

$$QV^c_{(\tau_{j-1},\tau_j]} = \int_{\tau_{j-1}}^{\tau_j} \sigma_s^2 ds, \qquad QV^d_{(\tau_{j-1},\tau_j]} = \int_{\tau_{j-1}}^{\tau_j}\int_{\mathbb{R}} x^2 \mu(ds, dx), \tag{5.6}$$

denotes the quadratic variation due to continuous and discontinuous price moves, respectively, for week j spanning the (τ_{j-1}, τ_j) time-interval. This split of the quadratic variation is directly motivated by the extensive recent literature on so-called realized volatility measures, which have documented very different dynamic dependencies in the two components; see, e.g., the empirical analysis in Andersen et al. (2007) building on the decompositions original developed by Barndorff-Nielsen and Shephard (2004, 2006). In the results reported on below, we follow Bollerslev and Todorov (2011b) in the use of five-minute S&P 500 futures prices and so-called truncated variation measures for empirically quantifying $QV^c_{(\tau_{j-1},\tau_j]}$ and $QV^d_{(\tau_{j-1},\tau_j]}$. The $\epsilon_j^{\pm}$ error term in (5.5) essentially reflects information in the tail index not

[26] The use of AR(1) type models for characterizing the dynamic dependencies in the tail index parameters has previously been explored from a very different perspective by Wagner (2005).

contained in the linear span of $\log(1+QV^c_{(\tau_{j-1},\tau_j]})$ and $\log(1+QV^d_{(\tau_{j-1},\tau_j]})$.[27]

In order to estimate the parameters of the model, we will further assume that the $\epsilon^{\pm}_j$ error terms are conditionally median unbiased; i.e., $\text{med}_{\tau_{j-1}}(\epsilon^{\pm}_j)=0$. All of the β parameters, say $\underline{\beta}^{\pm}$, may then be estimated by combining the previous nonparametric weekly tail index estimates with the corresponding full-sample objective function and specific parametric model structure in (5.5). Specifically,

$$\begin{aligned}\widehat{\underline{\beta}}^{\pm} = \text{argmin}_{\underline{\beta}^{\pm}} \sum_{j=1}^{J}\sum_{t=\tau_{j-1}}^{\tau_j}\frac{1}{N^{\pm}_t}\sum_{i=2}^{N^{\pm}_t} g\Big(\frac{\log\left(\frac{O_{t,\tau_t}(k_{t,i})}{O_{t,\tau}(k_{t,i-1})}\right)}{k_{t,i}-k_{t,i-1}} \\ - \Big(1-\beta^{\pm}_0-\beta^{\pm}_1\widehat{\alpha}^{\pm}_{j-1}-\beta^{\pm}_2\log(1+QV^c_{(\tau_{j-1},\tau_j]})-\beta^{\pm}_3\log(1+QV^d_{(\tau_{j-1},\tau_j]})\Big)\Big),\end{aligned} \tag{5.7}$$

where $\{\widehat{\alpha}^{\pm}_j\}_j$ refers to the weekly nonparametric estimates defined by (3.7). This objective function for the estimation of $\underline{\beta}^{\pm}$ mirrors the full-sample objective function for $\alpha^{\pm}$ in (3.5) obtained by replacing time-varying weekly $\alpha^{\pm}_j$s with their conditional median values implied by the model in (5.5).[28]

We begin by estimating the model in its most general form. We then sequentially omit any coefficients that are insignificant at the usual 5% level when judged by their individual t-statistics, starting with the numerically smallest. The resulting parameter estimates for the full and preferred models for each of the two tails are reported in Table 2. Focussing on the preferred specification, both of the autoregressive $\beta^{\pm}_1$ parameters are highly statistically significant, with the right tail showing the strongest own serial correlation. Accounting for the influence of the past tail index parameters and the past continuous variation, the past variation associated with jumps does not help explain the temporal variation in $\alpha^{\pm}_j$ for either of the two tails. Interestingly, for the right tail the past continuous variation and the β^{+}_2

[27] Assuming $|\beta^{\pm}_1|<1$, the parametric model in (5.5) may alternatively be expressed as,

$$\alpha^{\pm}_j-\frac{\beta^{\pm}_0}{1-\beta^{\pm}_1}-\frac{\beta^{\pm}_2}{1-\beta^{\pm}_1 L}\log(1+QV^c_{(\tau_{j-1},\tau_j]})-\frac{\beta^{\pm}_3}{1-\beta^{\pm}_1 L}\log(1+QV^d_{(\tau_{j-1},\tau_j]})=\frac{1}{1-\beta^{\pm}_1 L}\epsilon^{\pm}_j,$$

where L denotes the discrete time-shift (lag) operator. This allows for a direct test for the significance of the error term, by testing for serial correlation in the sample analogue of the expression on the left-hand-side. We will not pursue this idea any further here.

[28] A more complicated instrumental variable type LAD estimator could possibly be developed to help alleviate the potential errors-in-variables problem associated with the use of $\widehat{\alpha}^{\pm}_{j-1}$ and the high-frequency based estimates for $QV^c_{(\tau_{j-1},\tau_j]}$ and $QV^d_{(\tau_{j-1},\tau_j]}$ in place of their true values. We leave this for future research.

parameter also becomes insignificant once β_3^+ is fixed at zero, so that the preferred model reduces to a simple AR(1) structure. By contrast, $\hat{\beta}_2^-$ is significantly negative, implying that an increase in the continuous price variation for the S&P 500 market portfolio results in a fattening of the corresponding risk-neutral left jump tail.

The resulting weekly time series estimates for $1/\alpha_j^{\pm}$ are plotted in Figure 7. Although the model-based estimates are "smother" than the "raw" nonparametric weekly estimates implied by the confidence bounds in Figures 3 and 4, the estimates for the left jump tail, in particular, still exhibit substantial temporal variation, with dramatically higher values during periods of market distress. Of course, as previously noted, the overall magnitude of the risk-neutral left jump tail also far exceed that of the the right jump tail. Even though the autoregressive β_1^+ parameter for the right tail is highly significant, the fitted values of $1/\alpha_j^+$ remain within a fairly narrow range between 0.01 and 0.03 over the whole sample. By contrast, the fitted values of $1/\alpha_j^-$ for the left tail range from a low of 0.05 during "quiet" times to a high of 0.23 at the height of the 2008-09 financial crisis.[29]

6 Conclusion

We provide a new framework for estimating the shape of the risk-neutral jump tails, and the time-variation therein, based on a cross-section of short-maturity options. Our empirical results for the S&P 500 market portfolio point to nontrivial temporal dependencies in both of the tails, but especially so for the left tail, which fattens considerably during periods of market distress and financial crisis. Accounting for these changes in the shape of the jump tails is crucially important for satisfactorily explaining the observed dynamics of the short-maturity option surface. Our explicit modeling of the time-varying tail shapes further suggests that the higher the diffusive volatility of the market, the fatter the risk-neutral left jump tail. However, our parametric modeling also suggests that for neither of the tails is the temporal variation fully explained by the underlying market risks.

All of our results relate to the risk-neutral jump tails implied from the prices of options.

[29]Direct comparisons of the estimates obtained by the parametric models with the corresponding nonparametric estimates for the left and right tail indexes reveal a slight deterioration in the quality of the model fits during the recent financial crises, suggesting the scope for further improvements by incorporating other explanatory variables in addition to the quadratic variation of the jumps. Further details concerning these results are available on request.

It would be interesting to investigate whether similar dynamic dependencies carry over to the actually observed jump tails. In particular, could the option-implied tail estimates derived here be used for predicting rare tail events in the underlying market index? Or, does the apparent variation in the risk-neutral jump tails primarily stem from time-varying risk premia and/or changes in sentiment and attitude towards risk? Further along these lines, it would also be interesting to explore whether the new more flexible risk-neutral tail index estimates developed here could be used for actually predicting aggregate market returns. All of these questions seem worthy of future research.

Appendix

Lemma 1 *Suppose that the process X_t follows the dynamics in (2.2) under the risk-neutral measure $\mathbb{Q}$, where r_t and δ_t are deterministic, and the risk-neutral jump compensator is given by,*

$$\nu_t^{\mathbb{Q}}(dx) = \left(\phi_t^+ e^{-\alpha_t^+ x} 1_{\{x>0\}} + \phi_t^- e^{-\alpha_t^- |x|} 1_{\{x<0\}}\right) dx. \tag{A.1}$$

For $\phi_t^{\pm}$ and $\alpha_t^{\pm}$ assume that for some $\bar{t} > t$, we have

$$\mathbb{E}^{\mathbb{Q}}\left(|\phi_s^{\pm} - \phi_t^{\pm}|^2 \middle| \mathcal{F}_t\right) \leq \mathcal{K}_t |s-t|, \quad \mathbb{E}^{\mathbb{Q}}\left(|\alpha_s^{\pm} - \alpha_t^{\pm}|^2 \middle| \mathcal{F}_t\right) \leq \mathcal{K}_t |s-t|, \quad \forall\ s \in [t, \bar{t}], \tag{A.2}$$

where $\mathcal{K}_t$ is a $\mathcal{F}_t$-adapted finite-valued random variable. Further for some $\iota > 0$,[30]

$$\inf_{s\in[t,\bar{t}]} \alpha_s^- > \iota, \quad \inf_{s\in[t,\bar{t}]} \alpha_s^+ > 3+\iota, \quad \sup_{s\in[t,\bar{t}]} \mathbb{E}^{\mathbb{Q}}\left(|\phi_s^{\pm}|^{3/2}\right) + \sup_{s\in[t,\bar{t}]} \mathbb{E}^{\mathbb{Q}}\left(\frac{F_s}{F_t}\right)^{3+\iota} < \infty. \tag{A.3}$$

Then for $\tau \downarrow 0$,

$$\frac{e^{r_{t,\tau}} O_{t,\tau}(k)}{\tau F_{t-,\tau}} \xrightarrow{\mathbb{P}} \begin{cases} \frac{\phi_t^+ e^{k(1-\alpha_t^+)}}{\alpha_t^+(\alpha_t^+ - 1)}, & \text{if } k > 0, \\ \frac{\phi_t^- e^{k(1+\alpha_t^-)}}{\alpha_t^-(\alpha_t^- + 1)}, & \text{if } k < 0, \end{cases}, \qquad t = 1, ..., T, \tag{A.4}$$

with the above convergence holding uniformly in k over compact subsets of $(-\infty, 0) \cup (0, +\infty)$.

Proof of Lemma 1. We will only show the first part of (A.4), the second being shown in exactly the same way. We first collect some preliminary results and decompositions needed

[30] The condition on α_t^+ for the right tail ensures that the third moment of the arithmetic returns are finite. The left tail and the value of the α_t^- parameter play no role in the moment conditions.

for the proof of the Lemma. Since the limit in (A.4) is for $\tau \downarrow 0$, we will henceforth assume that $\tau < \bar{t}$, for $\bar{t}$ the constant appearing in (A.2) and (A.3).

Preliminary results and decompositions. Using the fact that by standard no-arbitrage pricing, $F_{t-,\tau} = X_{t-}e^{\int_t^{t+\tau}(r_s-\delta_s)ds}$, and recalling the assumption that r_t and δ_t are deterministic, we have

$$\frac{e^{r_{t,\tau}}C_{t,\tau}(k)}{\tau F_{t-,\tau}} = \frac{e^{r_{t,\tau}}\mathbb{E}_t^{\mathbb{Q}}\left(e^{-\int_t^{t+\tau}r_s ds}(X_{t+\tau}-K)\right)^+}{\tau F_{t-,\tau}} = \frac{1}{\tau}\mathbb{E}_t^{\mathbb{Q}}\left(e^{f_{t+\tau}-f_t}-e^k\right)^+, \tag{A.5}$$

where $f_t = \log(F_t)$ for F_t the futures price for X_t expiring at some future date not before τ (since we are interested in the increment $f_{t+\tau} - f_t$, the expiration of the futures does not matter as long as it is at or after τ), and $C_{t,\tau}(k)$ denotes the call price on X_t at time t with time-to-maturity τ and strike $K = F_{t-,\tau}e^k$. From the risk-neutral dynamics of X_t in (2.2), it follows by Itô 's formula that

$$df_t = -\frac{1}{2}\sigma_t^2 dt - \int_{\mathbb{R}}(e^x-1)\,\nu_t^{\mathbb{Q}}(dx)dt + \sigma_{t-}dW_t^{\mathbb{Q}} + \int_{\mathbb{R}} x\tilde{\mu}^{\mathbb{Q}}(dt,dx). \tag{A.6}$$

The jumps may be split into,

$$J_t^+ = \int_0^t\int_{x>0} x\mu^{\mathbb{Q}}(ds,dx) \qquad J_t^- = \int_0^t\int_{x<0} x\mu^{\mathbb{Q}}(ds,dx). \tag{A.7}$$

Using the Grigelionis representation theorem (Theorem 2.1.2 in Jacod and Protter, 2012), J_t^+ and J_t^- may alternatively be represented as,

$$\begin{aligned} J_t^+ &= \textstyle\int_0^t\int_{\mathbb{R}} \frac{\log(\phi_s^+/\alpha_s^+)-\log(y)}{\alpha_s^+}1_{\{0<y<\phi_s^+/\alpha_s^+\}}\underline{\mu}^+(ds,dy), \\ J_t^- &= \textstyle\int_0^t\int_{\mathbb{R}} \frac{\log(\alpha_s^-/\phi_s^-)+\log(y)}{\alpha_s^-}1_{\{0<y<\phi_s^-/\alpha_s^-\}}\underline{\mu}^-(ds,dy), \end{aligned} \tag{A.8}$$

where $\underline{\mu}^+$ and $\underline{\mu}^-$ are independent homogenous Poisson measures with compensators $\underline{\nu}^+(dt,dy) = dt\otimes dy$ and $\underline{\nu}^-(dt,dy) = dt\otimes dy$, respectively. We further denote,

$$\begin{aligned} \widetilde{J}_{t,\tau}^+ &= \textstyle\int_t^{t+\tau}\int_{\mathbb{R}} \frac{\log(\phi_t^+/\alpha_t^+)-\log(y)}{\alpha_t^+}1_{\{0<y<\phi_t^+/\alpha_t^+\}}\underline{\mu}^+(ds,dy), \\ \widetilde{J}_{t,\tau}^- &= \textstyle\int_t^{t+\tau}\int_{\mathbb{R}} \frac{\log(\alpha_t^-/\phi_t^-)+\log(y)}{\alpha_t^-}1_{\{0<y<\phi_t^-/\alpha_t^-\}}\underline{\mu}^-(ds,dy). \end{aligned} \tag{A.9}$$

Note that conditional on $\mathcal{F}_t$, $\widetilde{J}_{t,\tau}^+$ and $\widetilde{J}_{t,\tau}^-$ are the increments of Lévy processes with Lévy measures $\phi_t^+e^{-\alpha_t^+|x|}1_{\{x>0\}}ds\otimes dx$ and $\phi_t^-e^{-\alpha_t^-|x|}1_{\{x<0\}}ds\otimes dx$. Using this notation, further define,

$$z_{t,\tau} = \widetilde{J}_{t,\tau}^+ + \widetilde{J}_{t,\tau}^-, \qquad r_{t,\tau} = f_{t+\tau} - f_t - z_{t,\tau}. \tag{A.10}$$

Note that conditional on $\mathcal{F}_t$, $z_{t,\tau}$ is the increment of a double exponential Lévy process with characteristics that depend on $\mathcal{F}_t$. Lastly, decompose the "residual" $r_{t,\tau}$ as $r_{t,\tau}(1)+r_{t,\tau}(2)+r_{t,\tau}(3)$, where

$$r_{t,\tau}(1) = -\int_t^{t+\tau} \frac{1}{2}\sigma_s^2 ds - \int_t^{t+\tau}\int_{\mathbb{R}} (e^x - 1 + x)\,\nu_s^{\mathbb{Q}}(dx)ds, \quad r_{t,\tau}(2) = \int_t^{t+\tau} \sigma_{s-} dW_s^{\mathbb{Q}}, \tag{A.11}$$

$$r_{t,\tau}(3) = J^+_{t+\tau} - J^+_t + J^-_{t+\tau} - J^-_t - \widetilde{J}^+_{t,\tau} - \widetilde{J}^-_{t,\tau}. \tag{A.12}$$

Proof of Lemma 1 (continued). In the proof we will let $\mathcal{K}_t$ denote some $\mathcal{F}_t$-adapted finite-valued random variable. We start with $r_{t,\tau}(1)$ that does not depend on τ. Direct integration implies

$$\begin{aligned}\int_t^{t+\tau}\int_{\mathbb{R}} (e^x - 1)\,\nu_s^{\mathbb{Q}}(dx)ds = &\int_t^{t+\tau} \phi_s^+ \left(\frac{1}{\alpha_s^+ - 1} - \frac{1}{\alpha_s^+} + \frac{1}{(\alpha_s^+)^2}\right) ds \\ &+ \int_t^{t+\tau} \phi_s^- \left(\frac{1}{\alpha_s^- + 1} - \frac{1}{\alpha_s^-} - \frac{1}{(\alpha_s^-)^2}\right) ds.\end{aligned} \tag{A.13}$$

Since $\alpha_t^+ > 3$, $\alpha_t^- > 0$, and $\mathbb{E}^{\mathbb{Q}}(|\phi_t^{\pm}|^{3/2}) < \infty$ by assumption (A.3), it follows that

$$\mathbb{Q}\left(|r_{t,\tau}(1)| > \frac{1}{3}\tau^{\iota}\middle|\mathcal{F}_t\right) \leq \mathcal{K}_t \tau^{3/2-\iota}, \quad \forall \iota > 0. \tag{A.14}$$

Further, using the Burkholder-Davis-Gundy inequality (see e.g., Protter, 2004) and $\mathbb{E}^{\mathbb{Q}}(|\sigma_t|^{3/2}) < \infty$, we have

$$\mathbb{Q}\left(|r_{t,\tau}(2)| > \frac{1}{3}\tau^{\iota}\middle|\mathcal{F}_t\right) \leq \mathcal{K}_t \tau^{3/2-\iota}, \quad \forall \iota > 0. \tag{A.15}$$

We turn next to $r_{t,\tau}(3)$. Since $\alpha_t^+ > 1$, we may write

$$\begin{aligned}\mathbb{E}_t^{\mathbb{Q}}|J^+_{t+\tau} - J^+_t - \widetilde{J}^+_{t,\tau}| \leq \mathcal{K}_t \int_t^{t+\tau} \mathbb{E}_t^{\mathbb{Q}} &\left\{\int_0^{\phi_s^+ \wedge \phi_t^+} \left[|\log(\phi_s^+/\alpha_s^+) - \log(\phi_t^+/\alpha_t^+)| + |\log(y)||\alpha_t^+ - \alpha_s^+|\right] dy\right\} ds \\ &+ \mathcal{K}_t \int_t^{t+\tau} \mathbb{E}_t^{\mathbb{Q}} \left\{\int_{\frac{\phi_t^+}{\alpha_t^+} \wedge \frac{\phi_s^+}{\alpha_s^+}}^{\frac{\phi_t^+}{\alpha_t^+} \vee \frac{\phi_s^+}{\alpha_s^+}} \left[|\log(\phi_t^+/\alpha_t^+)| + |\log(\phi_s^+/\alpha_s^+)| + |\log(y)|\right] dy\right\} ds.\end{aligned} \tag{A.16}$$

From here it follows by (A.2) (and similar analysis for $J^-_{t+\tau} - J^-_t - \widetilde{J}^-_{t,\tau}$) that

$$\mathbb{Q}\left(|r_{t,\tau}(3)| > \frac{1}{3}\tau^{\iota}\middle|\mathcal{F}_t\right) \leq \mathcal{K}_t \tau^{3/2-\iota}, \quad \forall \iota > 0. \tag{A.17}$$

Using the fact that conditional on $\mathcal{F}_t$, $\underline{\mu}^{\pm}$ are homogenous Poisson measures, we have

$$\mathbb{Q}\left(\left(\underline{\mu}^+\left([t,t+\tau],\ [0,\frac{\phi_t^+}{\alpha_t^+}]\right) + \underline{\mu}^-\left([t,t+\tau],\ [0,\frac{\phi_t^-}{\alpha_t^-}]\right)\right) > 1\middle|\mathcal{F}_t\right) \leq \mathcal{K}_t\tau^2\left(\frac{\phi_t^+}{\alpha_t^+} + \frac{\phi_t^-}{\alpha_t^-}\right)^2. \tag{A.18}$$

Denoting the set,

$$\Omega_{t,\tau}=\left\{\omega:|r_{t,\tau}|<\tau^{\iota}\bigcap\left(\underline{\mu}^{+}\left([t,t+\tau],\ [0,\frac{\phi_t^{+}}{\alpha_t^{+}}]\right)+\underline{\mu}^{-}\left([t,t+\tau],\ [0,\frac{\phi_t^{-}}{\alpha_t^{-}}]\right)\right)\leq 1\right\}, \tag{A.19}$$

for arbitrary small $\iota>0$ and combining the above results, we have altogether

$$\mathbb{Q}\left(\Omega_{t,\tau}^{c}|\mathcal{F}_t\right)\leq\mathcal{K}_t\tau^{3/2-\iota},\quad\forall\iota>0. \tag{A.20}$$

Next, by the Hölder inequality,

$$\mathbb{E}_t^{\mathbb{Q}}\left\{e^{f_{t+\tau}-f_t}1_{\{\Omega_{t,\tau}^{c}\}}\right\}\leq\left(\mathbb{E}_t^{\mathbb{Q}}\left(e^{(f_{t+\tau}-f_t)\frac{3-2\iota}{1-3\iota}}\right)\right)^{\frac{1-3\iota}{3-2\iota}}\left(\mathbb{Q}\left(\Omega_{t,\tau}^{c}|\mathcal{F}_t\right)\right)^{\frac{2+\iota}{3-2\iota}}, \tag{A.21}$$

$$\mathbb{E}_t^{\mathbb{Q}}\left\{e^{z_{t,\tau}}1_{\{\Omega_{t,\tau}^{c}\}}\right\}\leq\left(\mathbb{E}_t^{\mathbb{Q}}\left(e^{z_{t,\tau}\frac{3-2\iota}{1-3\iota}}\right)\right)^{\frac{1-3\iota}{3-2\iota}}\left(\mathbb{Q}\left(\Omega_{t,\tau}^{c}|\mathcal{F}_t\right)\right)^{\frac{2+\iota}{3-2\iota}}. \tag{A.22}$$

From here, taking into account the bound on $\mathbb{Q}\left(\Omega_{t,\tau}^{c}|\mathcal{F}_t\right)$ in (A.20), and the integrability condition in the Lemma, it follows that for every $\epsilon>0$ and some sufficiently small $\iota>0$,

$$\mathbb{P}\left(\left|\mathbb{E}_t^{\mathbb{Q}}\left\{\left(\frac{1}{\tau}\left(e^{f_{t+\tau}-f_t}-e^{k}\right)^{+}-\phi_t^{+}\frac{e^{k(1-\alpha_t^{+})}}{\alpha_t^{+}(1-\alpha_t^{+})}\right)1_{\{\Omega_{t,\tau}^{c}\}}\right\}\right|\geq\epsilon\right)\leq\mathcal{K}_t\frac{\tau^{\iota}}{\epsilon}, \tag{A.23}$$

$$\mathbb{P}\left(\left|\mathbb{E}_t^{\mathbb{Q}}\left\{\left(\frac{1}{\tau}\left(e^{z_{t,\tau}\pm\tau^{\iota}}-e^{k}\right)^{+}-\phi_t^{+}\frac{e^{k(1-\alpha_t^{+})}}{\alpha_t^{+}(1-\alpha_t^{+})}\right)1_{\{\Omega_{t,\tau}^{c}\}}\right\}\right|\geq\epsilon\right)\leq\mathcal{K}_t\frac{\tau^{\iota}}{\epsilon}. \tag{A.24}$$

Using the definition of the set $\Omega_{t,\tau}$,

$$\begin{aligned}\mathbb{E}_t^{\mathbb{Q}}\left\{\left(e^{f_{t+\tau}-f_t}-e^{k}\right)^{+}1_{\{\Omega_{t,\tau}\}}\right\}&\geq\mathbb{E}_t^{\mathbb{Q}}\left\{\left(e^{z_{t,\tau}-\tau^{\iota}}-e^{k}\right)^{+}1_{\{\Omega_{t,\tau}\}}\right\},\\ \mathbb{E}_t^{\mathbb{Q}}\left\{\left(e^{f_{t+\tau}-f_t}-e^{k}\right)^{+}1_{\{\Omega_{t,\tau}\}}\right\}&\leq\mathbb{E}_t^{\mathbb{Q}}\left\{\left(e^{z_{t,\tau}+\tau^{\iota}}-e^{k}\right)^{+}1_{\{\Omega_{t,\tau}\}}\right\}.\end{aligned} \tag{A.25}$$

Therefore, in view of (A.23)-(A.24), it suffices to show that

$$\frac{1}{\tau}\mathbb{E}_t^{\mathbb{Q}}\left\{\left(e^{z_{t,\tau}\pm\tau^{\iota}}-e^{k}\right)^{+}1_{\{\Omega_{t,\tau}\}}\right\}\ \xrightarrow{\mathbb{P}}\ \frac{\phi_t^{+}e^{k(1-\alpha_t^{+})}}{\alpha_t^{+}(\alpha_t^{+}-1)},\quad t=1,...,T, \tag{A.26}$$

uniformly in k. Using the fact that on the set $\Omega_{t,\tau}$ there is at most one jump, and further this jump should be positive for $e^{z_{t,\tau}\pm\tau^{\iota}}-e^{k}$ to be positive (provided τ is sufficiently small), it follows that

$$\begin{aligned}&\mathbb{E}_t^{\mathbb{Q}}\left\{\left(e^{z_{t,\tau}\pm\tau^{\iota}}-e^{k}\right)^{+}1_{\{\Omega_{t,\tau}\}}\right\}\\&=\mathbb{E}_t^{\mathbb{Q}}\left\{\int_t^{t+\tau}\int_0^{\frac{\phi_t^{+}}{\alpha_t^{+}}e^{-\alpha_t^{+}(k\mp\tau^{\iota})}}\left[\exp\left(\frac{\log(\phi_t^{+}/\alpha_t^{+})-\log(y)}{\alpha_t^{+}}\pm\tau^{\iota}\right)-e^{k}\right]\underline{\mu}^{+}(dy,ds)1_{\{\Omega_{t,\tau}\}}\right\}.\end{aligned} \tag{A.27}$$

By the Burkholder-Davis-Gundy inequality as well as the Hölder inequality, (A.20), and the fact that $\alpha_t^+ > 1$,

$$\begin{aligned}
&\mathbb{E}_t^{\mathbb{Q}}\left\{\int_t^{t+\tau}\int_0^{\frac{\phi_t^+}{\alpha_t^+}e^{-\alpha_t^+(k\mp\tau^\iota)}}\left[\exp\left(\frac{\log(\phi_t^+/\alpha_t^+)-\log(y)}{\alpha_t^+}\pm\tau^\iota\right)-e^k\right]\underline{\mu}^+(dy,ds)1_{\{\Omega_{t,\tau}^c\}}\right\}\\
&\leq \mathcal{K}_t\left\{\mathbb{E}_t^{\mathbb{Q}}\left(\int_t^{t+\tau}\int_0^{\frac{\phi_t^+}{\alpha_t^+}e^{-\alpha_t^+(k\mp\tau^\iota)}}\left[\exp\left(\frac{\log(\phi_t^+/\alpha_t^+)-\log(y)}{\alpha_t^+}\pm\tau^\iota\right)-e^k\right]\underline{\mu}^+(dy,ds)\right)^{\alpha_t^+-\iota}\right\}^{1/(\alpha_t^+-\iota)}\\
&\quad\times\left(\mathbb{Q}\left(\Omega_{t,\tau}^c|\mathcal{F}_t\right)\right)^{1-1/(\alpha_t^+-\iota)}\\
&\leq\ \mathcal{K}_t\tau^{1+(1/2-\iota)(1-1/(\alpha_t^+-\iota))}.
\end{aligned}\tag{A.28}$$

Therefore, to prove (A.26), we need to show that

$$\begin{aligned}
&\mathbb{E}_t^{\mathbb{Q}}\left(\int_t^{t+\tau}\int_0^{\frac{\phi_t^+}{\alpha_t^+}e^{-\alpha_t^+(k\mp\tau^\iota)}}\left[\exp\left(\frac{\log(\phi_t^+/\alpha_t^+)-\log(y)}{\alpha_t^+}\pm\tau^\iota\right)-e^k\right]\underline{\mu}^+(dy,ds)\right)\\
&\qquad\xrightarrow{\mathbb{P}}\ \frac{\phi_t^+e^{k(1-\alpha_t^+)}}{\alpha_t^+(\alpha_t^+-1)},\quad t=1,...,T.
\end{aligned}\tag{A.29}$$

However, by direct calculations,

$$\begin{aligned}
&\mathbb{E}_t^{\mathbb{Q}}\left\{\int_t^{t+\tau}\int_0^{\frac{\phi_t^+}{\alpha_t^+}e^{-\alpha_t^+(k\mp\tau^\iota)}}\left[\exp\left(\frac{\log(\phi_t^+/\alpha_t^+)-\log(y)}{\alpha_t^+}\pm\tau^\iota\right)-e^k\right]\underline{\mu}^+(dy,ds)\right\}\\
&=\tau\mathbb{E}_t^{\mathbb{Q}}\left\{\int_0^{\frac{\phi_t^+}{\alpha_t^+}e^{-\alpha_t^+(k\mp\tau^\iota)}}\left[\exp\left(\frac{\log(\phi_t^+/\alpha_t^+)-\log(y)}{\alpha_t^+}\pm\tau^\iota\right)-e^k\right]dy\right\}\\
&=\tau\phi_t^+e^{\pm\alpha_t^+\tau^\iota}\left[\frac{e^{k(1-\alpha_t^+)}}{(\alpha_t^+-1)}-\frac{e^{k(1-\alpha_t^+)}}{\alpha_t^+}\right],
\end{aligned}\tag{A.30}$$

from which the result in (A.29), and hence (A.4), trivially follows. □

Tables and Figures

Table 1: Available Options as a Function of Moneyness

$\frac{K}{F_t}$	< 0.9	$(0.9, 0.9125)$	$(0.9125, 0.925)$	$(1.05, 1.0625)$	$(1.0625, 1.075)$	> 1.075
	18.21	1.88	1.97	1.84	1.48	5.51
$\frac{\log(K/F_t)}{\sigma_t^{ATM}\sqrt{\tau_t}}$	< -3.0	$(-2.5, -3)$	$(-2.0, -2.5)$	$(1.0, 1.25)$	$(1.25, 1.5)$	> 1.5
	15.51	2.69	2.95	2.03	1.94	5.67

Note: The table reports the average number of options available per trading day for different moneyness categories. σ_t^{ATM} refers to the day t at-the-money Black-Scholes implied volatility.

Table 2: Model Parameter Estimates

	β_0^-	β_1^-	β_2^-	β_3^-
α_j^-	12.783 (0.327)	0.350 (0.015)	-2.110 (0.099)	-0.001 (0.194)
	12.784 (0.323)	0.350 (0.014)	-2.110 (0.099)	$-$
	β_0^+	β_1^+	β_2^+	β_3^+
α_j^+	-1.519 (1.385)	0.861 (0.015)	4.277 (0.420)	-0.631 (0.611)
	23.191 (0.683)	0.562 (0.011)	$-$	$-$

Note: The table reports the parameter estimates for model in equation (5.5) for the weekly tail shape parameters $\alpha_j^{\pm}$, with asymptotic standard errors in parentheses. Separate model estimates are reported for the left tails (top panel) and right tails (bottom panel).

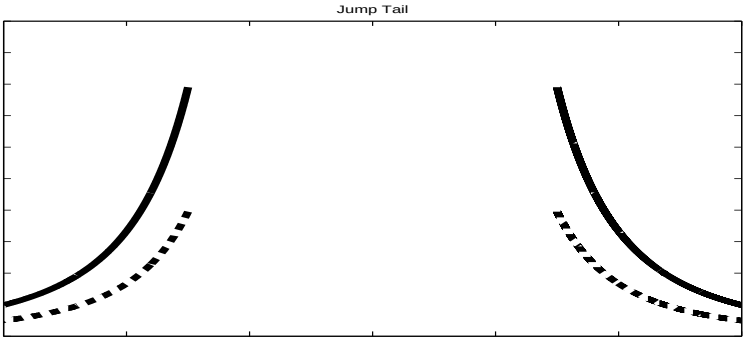

Figure 1: *Jump Tail Intensity for Different Level Shift Parameters.* The figure plots the jump tail intensity $\nu_t^{\mathbb{Q}}(dx)$ defined in equation (2.7) for different values of the $\phi_t^{\pm}$ parameters.

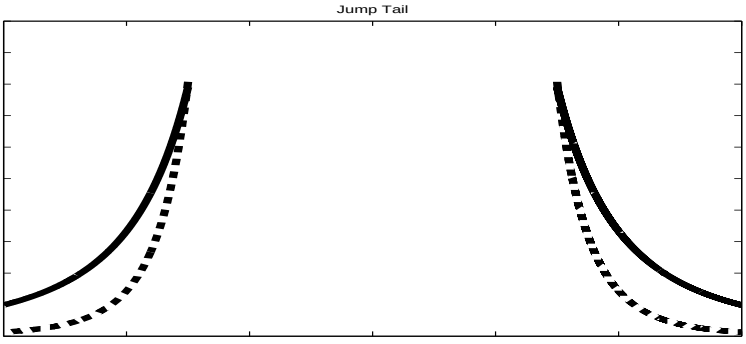

Figure 2: *Jump Tail Intensity for Different Shape Parameters.* The figure plots the jump tail intensity $\nu_t^{\mathbb{Q}}(dx)$ defined in equation (2.14) for different values of the tail decay parameter $\alpha_t^{\pm}$.

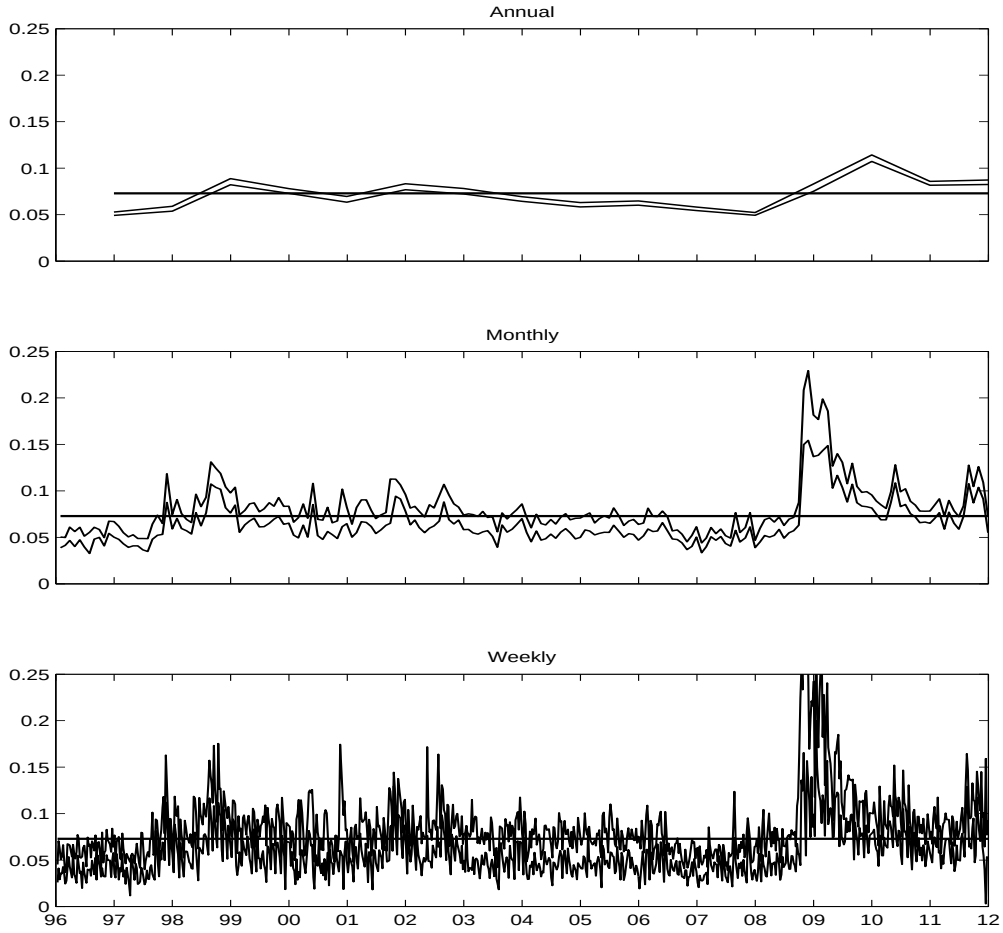

Figure 3: *Left Jump Tail Index Estimates.* The figure plots 95% confidence bands for the estimates of $1/\alpha_t^-$ under the assumption that the shape of the left jump tails are constant over annual (top), monthly (middle), and weekly (bottom) horizons, respectively. The calculation of the confidence bounds explicitly adjust for the presence of first-order spatial dependence in the estimates.

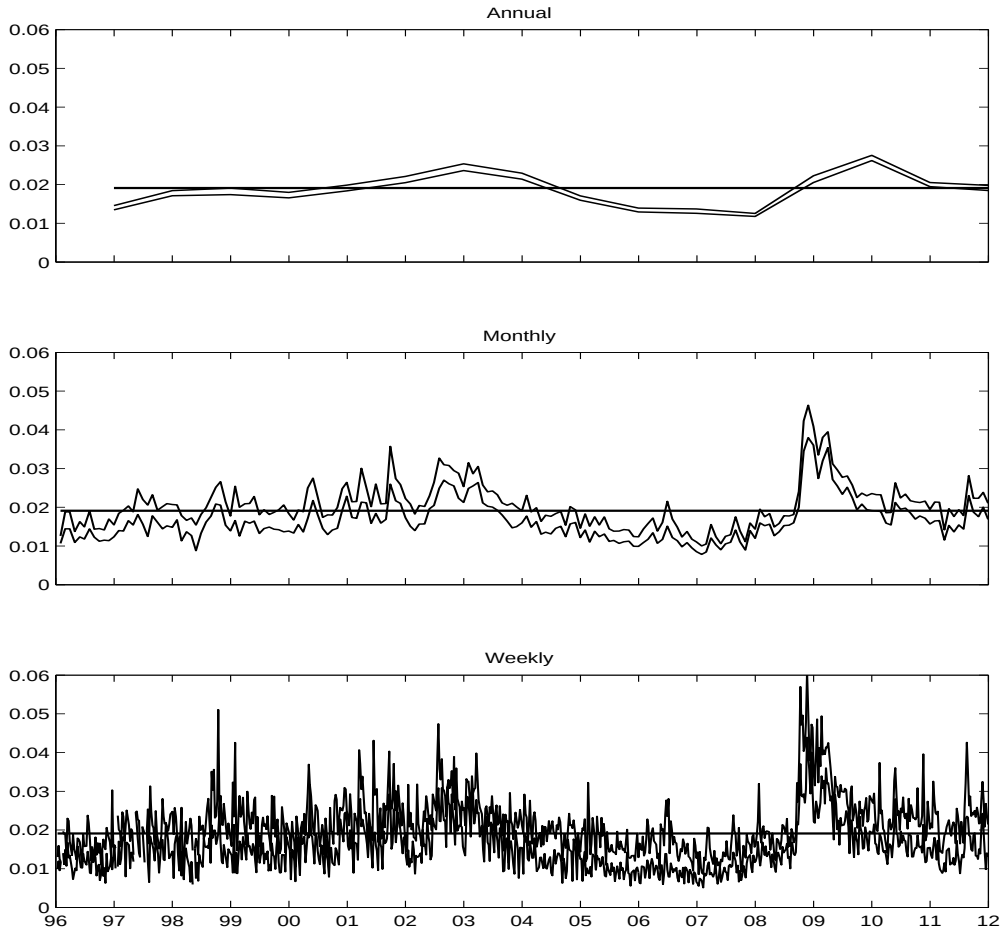

Figure 4: *Right Jump Tail Index Estimates.* The figure plots 95% confidence bands for the estimates of $1/\alpha_t^+$ under the assumption that the shape of the right jump tails are constant over annual (top), monthly (middle), and weekly (bottom) horizons, respectively. The calculation of the confidence bounds explicitly adjust for the presence of first-order spatial dependence in the estimates.

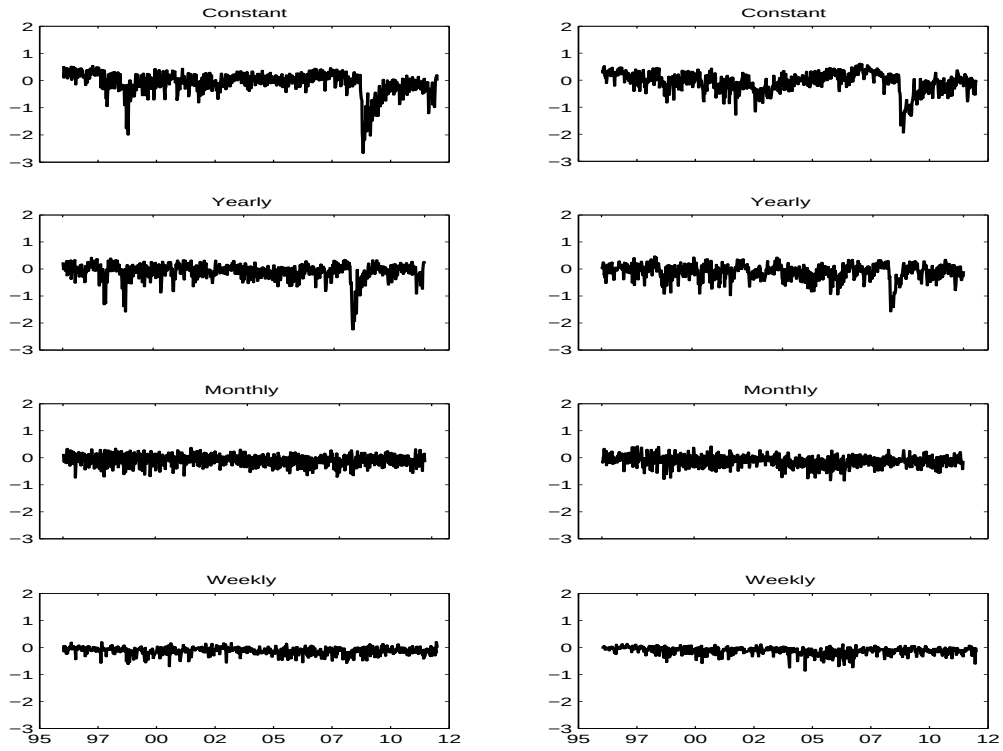

Figure 5: *Relative Option Tail Estimation Errors.* The figure plots the relative fit of the $\log(O_{t,\tau_t}(k_{t,1})/O_{t,\tau_t}(k_{t,N_t^{\pm}}))$ ratio averaged over weeks, under the assumption that the tail index parameters are constant over the whole sample, annual, monthly, and weekly horizons, respectively. The left (right) panels report the fits for the puts (calls) and the left (right) tails.

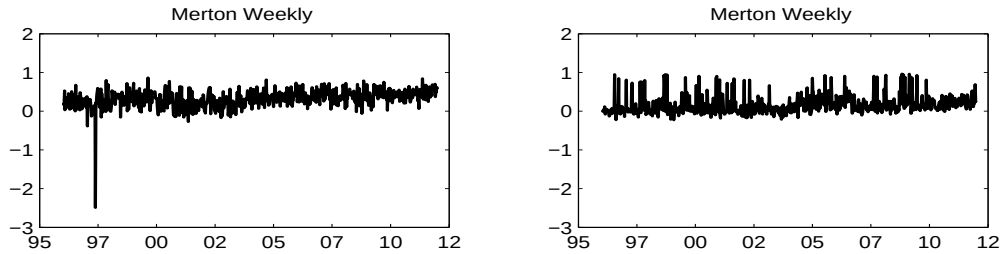

Figure 6: *Relative Option Tail Estimation Errors for the Merton Jump Model.* The figure plots the relative fit of the $\log(O_{t,\tau_t}(k_{t,1})/O_{t,\tau_t}(k_{t,N_t^{\pm}}))$ ratio from the Merton jump model estimated on a weekly basis. The left (right) panel reports the fits for the puts (calls) and the left (right) tails.

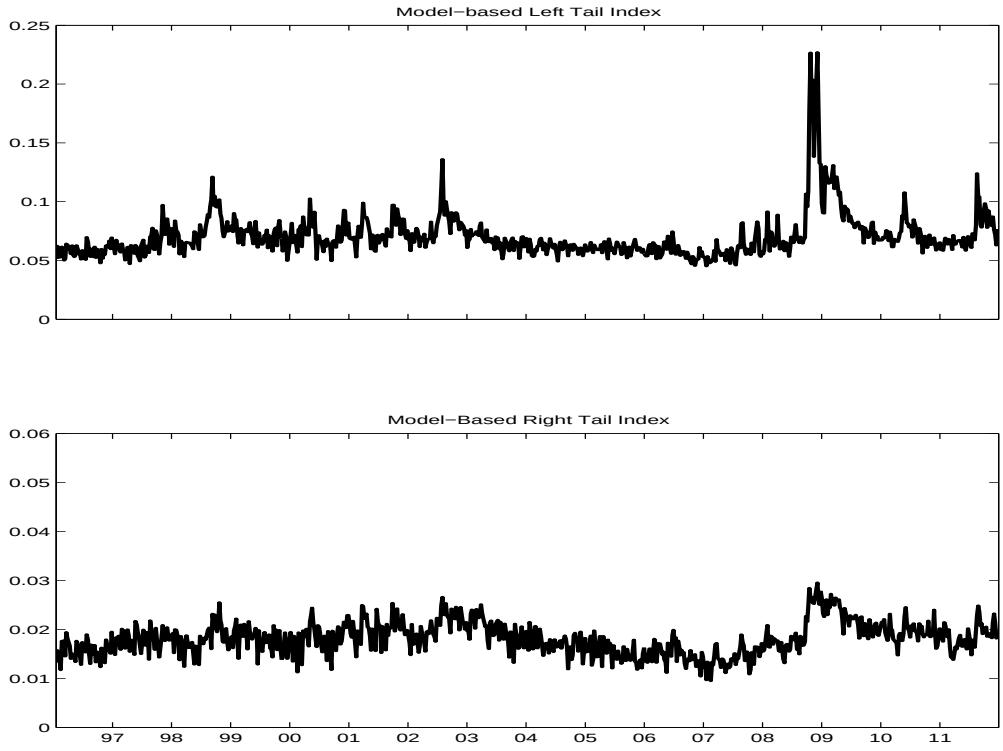

Figure 7: *Model-based Jump Tail Index Estimates.* The figure plots the fitted values of the left (top) and right (bottom) tail indexes, $1/\alpha_j^-$ and $1/\alpha_j^+$, respectively, based on the parametric model in equation (5.5).

References

Aït-Sahalia, Y., M. Karaman, and L. Mancini (2013). The Term Structure of Variance Swaps, Risk Premia and the Expectations Hypothesis. Princeton University, Working paper.

Aït-Sahalia, Y. and A. Lo (1998). Nonparametric Estimation of State-Price Densities Implicit in Financial Asset Prices. *Journal of Finance 53*, 499–548.

Andersen, T. G., L. Benzoni, and J. Lund (2002). An Empirical Investigation of Continuous-Time Equity Return Models. *Journal of Finance 57*, 1239–1284.

Andersen, T. G. and T. Bollerslev (1998). Answering the Skeptics: Yes, Standard Volatility Models do Provide Accurate Forecasts. *International Economic Review 39*, 885–905.

Andersen, T. G., T. Bollerslev, and F. X. Diebold (2007). Roughing It Up: Including Jump Components in the Measurement, Modeling, and Forecasting of Return Volatility. *Review of Economics and Statistcis 89*, 701–720.

Andersen, T. G., T. Bollerslev, F. X. Diebold, and L. P. (2001). The Distribution of Realized Exchange Rate Volatility. *Journal of the American Statistical Association 42*, 42–55.

Andersen, T. G., N. Fusari, and V. Todorov (2013). Parametric Inference and Dynamic State Recovery from Option Panels. Working paper, Northwstern University.

Barndorff-Nielsen, O. E. and N. Shephard (2002). Econometric Analysis of Realised Volatility and its use in Estimating Stochastic Volatility Models. *Journal of the Royal Statistical Society, Series B 64*, 253–280.

Barndorff-Nielsen, O. E. and N. Shephard (2004). Power and Bipower Variation with Stochastic Volatility and Jumps. *Journal of Financial Econometrics 2*, 1–37.

Barndorff-Nielsen, O. E. and N. Shephard (2006). Econometrics of Testing for Jumps in Financial Economics using Bipower Variation. *Journal of Financial Econometrics 4*, 1–30.

Barro, R. J. (2006). Rare Disasters and Asset Markets in the Twentieth Century. *Quarterly Journal of Economics 121*, 823–866.

Bates, D. S. (1996). Jumps and Stochastic Volatility: Exchange Rate Processes Implicit in Deutsche Mark Options. *Review of Financial Studies 9*, 69–107.

Bates, D. S. (2000). Post-'87 Crash Fears in S&P 500 Future Options. *Journal of Econometrics 94*, 181–238.

Bhargava, A. (2013). Executive Compensation, Share Repurchases and Investment Expenditures: Econometric Evidence from US Firms. *Review of Quantitative Finance and Accounting 40*, 403–422.

Bollerslev, T. and V. Todorov (2011a). Estimation of Jump Tails. *Econometrica 79*, 1727–1783.

Bollerslev, T. and V. Todorov (2011b). Tails, Fears and Risk Premia. *Journal of Finance 66*, 2165–2211.

Broadie, M., M. Chernov, and M. Johannes (2007). Specification and Risk Premiums: The Information in S&P 500 Futures Options. *Journal of Finance 62*, 1453–1490.

Carr, P., H. Geman, D. Madan, and M. Yor (2003). Stochastic Volatility for Lévy Processes. *Mathematical Finance 13*, 345–382.

Christoffersen, P., K. Jacobs, and C. Ornthanalai (2012). Dynamic Jump Intensities and Risk Premiums: Evidence from S&P 500 Returns and Options. *Journal of Financial Economics 106*, 447–472.

Cont, R. and P. Tankov (2004). *Financial Modelling with Jump Processes*. Boca Raton, Florida: Chapman and Hall.

Duffie, D. (2001). *Dynamic Asset Pricing Theory* (3rd ed.). Princeton, New Jersey: Princeton University Press.

Duffie, D., J. Pan, and K. Singleton (2000). Transform Analysis and Asset Pricing for Affine Jump-Diffusions. *Econometrica 68*, 1343–1376.

Embrechts, P., C. Kluppelberg, and T. Mikosch (2001). *Modelling Extremal Events* (3rd ed.). Berlin: Springer-Verlag.

Eraker, B. (2004). Do Stock Prices and Volatility Jump? Reconciling Evidence from Spot and Option Prices. *Journal of Finance 59*, 1367–1403.

Gabaix, X. (2012). Variable Rare Disasters: An Exactly Solved Framework for Ten Puzzles in Macro-Finance. *Quarterly Journal of Economics 127*, 645–700.

Galbraith, J. W. and S. Zernov (2004). Cricuit Breakers and the Tail Index of Equity Returns. *Journal of Financial Econometrics 2*, 109–129.

Hamidieh, K. (2011). Estimating the Tail Shape Parameter from Options Data. California State University at Fullerton, Working paper.

Jacod, J. (1979). *Calcul Stochastique et Problèmes de Martingales*. Lecture notes in Mathemtatics 714. Berlin: Springer-Verlag.

Jacod, J. and P. Protter (2012). *Discretization of Processes*. Berlin: Springer-Verlag.

Jacod, J. and A. N. Shiryaev (2003). *Limit Theorems For Stochastic Processes* (2nd ed.). Berlin: Springer-Verlag.

Kelly, B. (2012). Tail Risk and Asset Prices. University of Chicago, Working paper.

Kou, S. (2002). A Jump Diffusion Model for Option Pricing. *Management Science 48*, 1086–1101.

Kou, S. and H. Wang (2002). Option Pricing under a Double Exponential Jump Diffusion Model. *Management Science 50*, 1178–1192.

Merton, R. (1976). Option Pricing when Underlying Asset Returns are Discontinuous. *Journal of Financial Economics 3*, 125–144.

Metaxoglou, K. and A. Smith (2012). State Prices of Conditional Quantiles: New Evidence on Time Variation in the Pricing Kernel. University of California, Davis, Working paper.

Pan, J. (2002). The Jump-Risk Premia Implicit in Options: Evidence from an Integrated Time-Series Study. *Journal of Financial Economics 63*, 3–50.

Protter, P. (2004). *Stochastic Integration and Differential Equations* (2nd ed.). Berlin: Springer-Verlag.

Quintos, C., Z. Fan, and P. C. B. Phillips (2001). Structural Change Tests in Tail Behavior and the Asian Crisis. *Review of Economic Studies 68*, 633–663.

Rietz, T. (1988). The Equity Risk Premium: A Solution. *Journal of Monetary Economics 22*, 117–131.

Rosenberg, J. and R. Engle (2002). Empirical Pricing Kernels. *Journal of Financial Economics 64*, 342–372.

Rubinstein, M. (1994). Implied Binomial Trees. *Journal of Finance 69*, 771–817.

Song, Z. and D. Xiu (2013). A Tale of Two Option Markets: Pricing Kernels and Volatility Risk. University of Chicago, Working paper.

Wachter, J. A. (2013). Can Time-Varying Risk of Rare Disasters Explain Aggregate Stock Market Volatility? *Journal of Finance*. forthcoming.

Wagner, N. (2005). Autoregressive Conditional Tail Behavior and Results on Government Bond Yield Spreads. *International Review of Financial Analysis 14*, 247–261.